

# **POLITECNICO DI TORINO**

Corso di Laurea Magistrale

in Ingegneria per l'Ambiente e il Territorio

Tesi di Laurea Magistrale

Persitence of peroxydisulfate in aquifer material



**Relatore**

Ing. Tiziana Tosco

**Correlatore**

Ing. Lenka Honetschlägerová

**Candidata**

Luciana Summa



## Abstract

In the last ten years the peroxydisulfate (PDS) application as oxidant for in-situ chemical oxidation (ISCO) technology became popular for remediation of contaminated soil and groundwater. Due to its high oxidation potential, PDS has a high capacity to degrade a wide variety of contaminants. However, due to its low use, limited information is still available about stability, persistence, and transport. The objective of this study was to identify the stability of unactivated PDS in presence of two soils from Czech Republic and a sea sand. Degradation rate coefficients and half-life were analyzed and the dependence on total organic carbon (TOC) and inorganic elements content, such as Fe and Mn, was studied. A series of batch and column experiments were performed to estimate the changes in PDS concentration over time. Batch experiments were conducted in triplicates in a system containing 100 g of solids at 1 or 20 g/L of PDS. Column experiments were performed injecting PDS with constant flowrate (5 mL/min) at high concentration (20 g/L) into the columns containing natural soil or sea sand. PDS changes were analyzed studying breakthrough curves (temporal evolution of PDS concentration in the effluent). The decomposition of PDS followed the first-order rate law for all aquifer materials investigated and was strongly related to TOC and Fe content. For the soil with higher TOC content, the decomposition was faster with an exponential decay over time. On the other hand, in absence of organic carbon, there was no evident reaction with PDS. Column experiments gave information about decomposition and transport of PDS showing that for the soil with high TOC content there was an evident reactivity with PDS. The soil with no TOC and Fe content, quickly reached the influent concentration showing an absence of reaction with PDS. The results showed that TOC and Fe content played an important role in PDS loss and the study of these properties were able to give information about persistence and stability of PDS.

# Contents

1	Introduction .....	14
2	Theoretical part .....	16
2.1	Contaminated sites - general background .....	16
2.2	Overview of the most common contaminated sites .....	16
2.3	In situ chemical oxidation .....	22
2.3.1	ISCO reactants.....	24
2.4	Peroxydisulfate.....	28
2.4.1	Mechanisms of PDS reactions.....	28
2.4.2	Free radical scavengers affecting peroxydisulfate oxidation .....	34
2.4.3	Persistence of unactivated PDS in the presence of aquifer solids.....	36
2.4.4	Persistence of activated peroxydisulfate in the presence of aquifer solids .....	41
2.4.5	Fundamentals using PDS – A resume .....	42
3	Materials and methods .....	44
3.1	Chemicals .....	44
3.2	Aquifer materials.....	44
3.3	Soils characteristics .....	45
3.3.1	Determination of Different Forms of Carbon .....	45
3.3.2	Elemental composition.....	46
3.4	Spectrophotometric determination of sodium persulfate concentration .....	47
3.4.1	Calibration curve .....	48
3.4.1.1	Apparatus .....	49
3.4.1.2	Procedure .....	49
3.5	Batch experiments .....	50
3.5.1	PDS concentration.....	52
3.5.1.1	Dilutions.....	52

3.5.1.1.1	Controls .....	52
3.5.1.1.2	Soils reactors.....	53
3.6	Column experiments .....	55
3.7	Statistical analysis .....	58
4	Results and discussions .....	59
4.1	Properties and composition .....	59
4.1.1	Total Carbon.....	59
4.1.2	X-Ray Fluorescence analysis .....	60
4.2	Determination of PDS concentration .....	64
4.2.1	Calibration curve .....	64
4.2.2	Batch experiments .....	65
4.2.2.1	Control reactors.....	68
4.2.2.2	Sample reactors – Kinetic approach.....	69
4.2.2.2.1	Low PDS concentration.....	69
4.2.2.2.2	High PDS concentration .....	72
4.2.2.3	Sample reactors – SOD approach .....	75
4.3	Column experiments .....	78
4.4	Comparison with literature data .....	79
4.4.1	Batch experiments .....	79
4.4.2	Column experiments .....	85
5	Conclusions .....	87
6	References .....	89

## Abbreviations

Abbreviations	Meaning
Abs	Absorbance
C	Final PDS concentration
C <sub>0</sub>	Initial PDS concentration
CA	Citric acid
COD	Chemical Oxygen Demand
d	Days
DCE	Dichloroethane
DCM	Dichloromethane
DDT	Dichlorodiphenyltrichloroethane
DF	Dilution factor
DNAPL	Dense Non-Aqueous Phase Liquid
EEA	European Environmental Agency
EPA	United States Environmental Protection Agency
Eq.	Equation
Fig.	Figure
ISCO	In situ chemical oxidation
ISPRA	Istituto Superiore per la Protezione e la Ricerca Ambientale
k	Degradation rate coefficient
NOD	Natural Oxidant Demand

NOM	Natural Oxidant Demand
OCP	Organochlorines pesticides
PAH	Polycyclic Aromatic Hydrocarbon
PCB	Polychlorinated biphenyl
PCE	Perchloroethylene
PDS	Peroxydisulfate
PV	Pore volume
PVC	Polyvinyl chloride
Q	Flow-rate
R <sup>2</sup>	Correlation factor
ROC	Residual Oxidizable Carbon
SOM	Soil Oxidant Demand
t <sub>1/2</sub>	Half-life
Tab.	Table
TC	Total Carbon
TC	Trisodium citrate
TCA	Trichloroacetic acid
TCE	Trichloroethylene
TIC	Total Inorganic Carbon
TOC	Total Organic Carbon
VC	Vinyl chloride

VOC	Volatile Organic Compounds
XRF	X-Ray fluorescence
$\lambda$	Degradation rate coefficient
$\varepsilon$	Porosity

## List of Figures

Figure 1 - Sectors contributing to soil contamination in Europe (Journal of Environmental and Public Health, 2013).....	17
Figure 2 - Distribution of contaminants affecting soil and groundwater in Europe (Journal of Environmental and Public Health, 2013) .....	18
Figure 3 - Structure of PCE (wikipedia.org) .....	19
Figure 4 - Structure of TCE (wikipedia.org).....	19
Figure 5 - Schematic of chlorinated solvent pollution migrating downward in an aquifer (U.S. EPA 1999).....	21
Figure 6 - Structure of PCBs (researchgate.net) .....	22
Figure 7 - Delivery approaches .....	23
Figure 8 - Recirculation method used in ISCO (Interstate Technology and Regulatory Council, 2005).....	24
Figure 9 - ISCO using direct-push injection probes (ISCO for groundwater remediation, Siegrist et al (2011)) .....	24
Figure 10 - The depletion of chlorinated organic solvents by activated PDS at different temperature 30 °C, 40 °C, 50 °C (Liu et al. (2014)) .....	30
Figure 11 - Concentration of reactants vs time for a first-order reaction.....	37
Figure 12 - Soil 1.....	44
Figure 13 - Soil 2.....	45
Figure 14 - Sea sand .....	45
Figure 15 - George Dowell periodic table showing specific energy range for some elements	47
Figure 16 - Spectrophotometer principle .....	48
Figure 17 - Calibration solutions.....	50
Figure 18 - Batch reactors .....	51
Figure 19 - Mixed batch reactors .....	51
Figure 20 - Filter (0.45 µm).....	54

Figure 21 - Batches soil 2.....	54
Figure 22 – Centrifuge .....	55
Figure 23 - Column experiment .....	56
Figure 24 - PDS flow into the columns.....	57
Figure 25 - Soil 1 spectra, no filter.....	61
Figure 26 - Soil 1 spectra, with Al filter .....	61
Figure 27 - Soil 2 spectra, no filter.....	62
Figure 28 - Soil 2 spectra, with Al filter .....	62
Figure 29 - Soil 3 spectra, no filter.....	63
Figure 30 - Soil 3 spectra, with Al filter .....	63
Figure 31 – Calibration curve.....	64
Figure 32 - Sample 1 solutions after 5 days at 1 g/L PDS concentration .....	65
Figure 33 - Sample 1 solution after 5 days at 20 g/L PDS concentration .....	66
Figure 34 - Sample 2 solution after 5 days at 1 g/L PDS concentration .....	66
Figure 35 - Sample 2 solution after 5 days at 20 g/L PDS concentration .....	67
Figure 36 - Sample 3 solution after 5 days at 1 g/L PDS concentration .....	67
Figure 37 - Sample 3 solution after 5 days at 20 g/L PDS concentration .....	67
Figure 38 - Control reactors data referred to the three samples (s1, s2, s3) for the entire experiment duration (10 days). Data refers to 1 g/L PDS concentration. ....	68
Figure 39 – Control reactors data referred to the three samples (s1, s2, s3) for the entire experiment duration (10 days). Data refers to 20 g/L PDS concentration. ....	69
Figure 40 - PDS concentration profile for the three samples. PDS initial concentration 1 g/L	71
Figure 41 - PDS concentration profile for the three samples. PDS initial concentration 20 g/L .....	73
Figure 42 - PDS concentrations plotted in semi-log scale for soil 1 (s1) at low and high PDS initial concentration, 1 g/L and 20 g/L (1, 20) .....	74

Figure 43 - PDS concentrations plotted in semi-log scale for soil 2 (s2) at low and high PDS initial concentration, 1 g/L and 20 g/L (1, 20) .....	74
Figure 44 - PDS concentrations plotted in semi-log scale for soil 3 (s3) at low and high PDS initial concentration, 1 g/L and 20 g/L (1, 20) .....	75
Figure 45- TOC vs k correlation for 1 g/L PDS concentration respectively for the three soils. ....	76
Figure 46 - Fe vs k correlation for 1 g/L PDS concentration respectively for the three soils..	76
Figure 47 - Fe vs k correlation for 20 g/L PDS concentration respectively for the three soils.	77
Figure 48 - Breakthrough curves related to PDS degradation .....	78
Figure 49 – TOC vs k correlation for 1 g/L PDS concentration (Sra et al. (2010)).....	81
Figure 50 - TOC vs k correlation for 20 g/L PDS concentration (Sra et al. (2010)) .....	81
Figure 51 – Fe vs k correlation for 1 g/L PDS concentration (Sra et al. (2010)).....	82
Figure 52 – Fe vs k correlation for 20 g/L PDS concentration (Sra et al. (2010)).....	82
Figure 53 – Mn vs k correlation for 1 g/L PDS concentration (Sra et al. (2010)) .....	83
Figure 54 – Mn vs k correlation for 20 g/L PDS concentration (Sra et al. (2010)) .....	83
Figure 55 - Breakthrough curves from Sra et al. (2010) studies .....	86

## List of Tables

Table 1 - Total Organic Carbon content and half-life for 20 g/L PDS concentration in Sra et al. (2010) studies .....	40
Table 2 - Preparation of calibration solutions .....	49
Table 3 - Stock solutions for batch experiments for each sample (1, 2, 3) at 1 g/L and 20 g/L PDS concentration.....	50
Table 4 - Experiment design .....	52
Table 5 -Dilution factor (20 g/L).....	53
Table 6 - Dilution factor (1 g/L).....	53
Table 7 - Dilution factor (20 g/L).....	53
Table 8 - Dilution factor (1 g/L).....	54

Table 9 – Results of Total Carbon (TC), Total Organic Carbon (TOC), Residual Oxidizable Carbon (ROC), Total Inorganic Carbon (TIC) referred to the three analyzed samples (S1, S2, S3). Measure were conducted in triplicate (1, 2, 3) considering for the same sample three total weights. ....	59
Table 10 - Elemental composition obtained from XRF analysis in ppm .....	63
Table 11 - Calibration curve data .....	64
Table 12 - Control reactors data referred to the three samples (s1, s2, s3) respectively at 1 g/L and 20 g/L of PDS concentration (1c, 20c). Measures performed at zero time, after 5 and 10 days.....	68
Table 13 – Average of PDS concentration, Standard Deviation, $C/C_0$ and $C/C_0$ Standard Deviation for Sample 1 (1 g/L PDS concentration) .....	70
Table 14 - Average of PDS concentration, Standard Deviation, $C/C_0$ and $C/C_0$ Standard Deviation for Sample 2 (1 g/L PDS concentration) .....	70
Table 15 - Average of PDS concentration, Standard Deviation, $C/C_0$ and $C/C_0$ Standard Deviation for Sample 2 (1 g/L PDS concentration) .....	70
Table 16 - Average of PDS concentration, Standard Deviation, $C/C_0$ and $C/C_0$ Standard Deviation for Sample 1 (20 g/L PDS concentration). ....	72
Table 17 - Average of PDS concentration, Standard Deviation, $C/C_0$ and $C/C_0$ Standard Deviation for Sample 2 (20 g/L PDS concentration). ....	72
Table 18 - Average of PDS concentration, Standard Deviation, $C/C_0$ and $C/C_0$ Standard Deviation for Sample 3 (20 g/L PDS concentration). ....	72
Table 19 - Porosity values ( $\epsilon$ ) for soil 1 and soil 3 calculated for column experiments considering the volume of water ( $V_w$ ) occupied into the pores and the total volume of the column ( $V_T$ ).....	79
Table 20 - Aquifer materials characteristics and rate coefficient at low (1 g/L) and high (20 g/L) PDS concentration (Sra et al. (2010)) .....	79
Table 21 - Half-life Sra et al. (2010).....	80
Table 22 - SOD tests Brown et al. (2004) .....	84
Table 23 - Column properties.....	85

Table 24 - Porosity values ..... 85

# 1 Introduction

In-situ chemical oxidation (ISCO) has been applied for the remediation of groundwater and it consists in the injection of a chemical oxidant in subsurface for the transformation of contaminants into less harmful species <sup>1</sup>. Recently, ISCO became an efficient technology for the degradation of organic contaminants, using oxidants with a high oxidation potential. Among oxidants, permanganate ( $\text{MnO}_4^-$ ), ozone ( $\text{O}_3$ ), hydrogen peroxide ( $\text{H}_2\text{O}_2$ ) and peroxydisulfate (PDS) alone or in combination are used within ISCO <sup>2</sup>. Particularly, the persistence and the stability of the oxidant in the subsurface are important since these parameters affect the mobility of oxidant to contaminated zones in the subsurface <sup>3</sup>.

$\text{MnO}_4^-$  persists for long periods of time and its transport through porous media is characterized by long distances <sup>1</sup>. Its reaction with contaminants is rapid, but the formation of Mn oxides leads to the clogging of pores and inhibits the transport of the oxidant <sup>4</sup>. Moreover, the reaction with natural organic matter (NOM) and metals may limit its application, leading to an increase in soil oxidant demand (SOD) expressed as “g oxidant/kg soil” <sup>5</sup>. ISCO using  $\text{O}_3$  involves the introduction of  $\text{O}_3$  as gas into the subsurface that due to its different reaction mechanism may degrade a great array of organic contaminants <sup>6</sup>. The treatment is effective because ozone can be delivered directly to the saturated zone and be effectively in contact with subsurface media. However,  $\text{O}_3$  being too unstable must be generated in situ and injected immediately when it is produced <sup>6</sup>.  $\text{H}_2\text{O}_2$  may persist in soil, but the diffusive and advective transport distances are limited: it decomposes quickly in the subsurface and is not able to decompose the contaminants far from the injection point <sup>4</sup>. A too fast reaction may limit the persistence and the capability of oxidant to degrade contaminants and in this way can impact on the total efficiency of the treatment <sup>3</sup>.

PDS is an oxidant recently introduced for ISCO, characterized by a high oxidation potential ( $E^0 = 2.6 \text{ V}$ ) and consequently a great capacity to react with a wide variety of organic compounds. The main characteristic is its capacity to be effective both when applied alone, or when activated (i.e., by thermal, metal ion, base activation). PDS activation generates radicals in order to have major oxidation potential. PDS is more stable and more mobile in subsurface than  $\text{MnO}_4^-$ . However, similarly to other strong oxidants, once injected <sup>7</sup> into the subsurface it does not react only with target contaminants, but also with soil constituents <sup>3</sup> that can lead to a rapid decomposition, limitation of the treatment area <sup>2</sup> and reduction of the mass of oxidant available for the destruction of contaminants <sup>8</sup>. For this reason, the investigation about soil constituents

is necessary in order to understand the relationships between PDS and soil and which species are more influential on PDS decomposition. The quantification of natural oxidant demand (NOD), related to the amount of PDS required to satisfy the natural consumption of PDS turns out fundamental in order to design cost-effective oxidant delivery systems, and more in general for a correct site-specific assessment<sup>8</sup>. Some studies have been conducted to evaluate the impact of TOC, Fe and Mn content on oxidation and PDS persistence. The latter was studied by Sra et al. (2010) in the case of unactivated PDS. Performing batch and column experiments, they demonstrated that first-order degradation coefficients depend upon TOC and Fe content of the investigated aquifer materials<sup>3</sup>. Particularly, soils with high TOC and Fe content have been shown to facilitate the decomposition of PDS and to impact its effectiveness and efficiency of the treatment<sup>2</sup>. Also, pH had a great relevance: a decrease in pH over time was observed, due to the production of H<sup>+</sup> with the use of PDS. High persistence of PDS will allow higher contact time for the oxidant transport, permitting advective and dispersive transport of PDS into subsurface<sup>3</sup>.

The general goal of this work was to identify the relevant aquifer material properties on which depend the stability and persistence of PDS. Knowing the main factors on which PDS decomposition depends, the aim was to identify the stability of unactivated PDS analyzing its consumption from the reaction with aquifer constituents.

In the first chapter an introduction about contaminated sites and ISCO technology is described, highlighting the more used reactants for the chemical oxidation. Also, an overview about the most contaminated sites is presented as a background to better understand the following sections. In material and methods, three representative samples (two soils from Czech Republic and a sea sand) and their properties are defined. In detail, in chapter 3.5 batch experiments are described in order to identify kinetic parameters and column experiments, described in chapter 3.6, are illustrated to represent PDS decomposition under in situ conditions. Some studies about unactivated PDS were identified in order to compare literature data with this work and evaluate the difference on soil properties and in detail on PDS decomposition, its stability and transport. Particularly, in chapter 4.4.1 batch experiments from Sra et al. (2010) study are evaluated and the correlation between degradation rate coefficient and soil constituents are represented. In chapter 4.4.2 breakthrough curves trend obtained from column experiments in literature are reported.

## 2 Theoretical part

### 2.1 Contaminated sites - general background

The term contamination is related to the presence of any (physical, chemical or biological) agent in a site in forms and concentrations that could damage the environment and the human health <sup>1</sup>. In order to manage the contamination, it is necessary to define two fundamental conditions <sup>2</sup>:

- Contaminated site refers to a well-defined area where the presence of soil contamination has been confirmed and represents a potential risk to humans, water, ecosystems and other receptors;
- Potentially contaminated site refers to sites where soil contamination is suspected but not verified and detailed investigations are still needed to verify whether there is unacceptable risk of adverse impacts on receptors.

The United States Environmental Protection Agency (EPA) and Italian National System for Environmental Protection (ISPRA), define two different categories of pollution: point-source contamination and diffuse contamination.

Point-source contamination is defined as any contamination that enters the environment from an easily identified and confined point source. Typically, a point-source contamination is characterized by high pollutant concentrations in a limited area, that eventually produces a wider contamination at lower concentration. On the other hand, the diffuse contamination does not have a defined entry point, the pollutants are released in a wide area and it is harder to identify and address it. Point sources derive typically from industry, urban or runoff due to industrial spills but diffuse contamination is most widespread such as the runoff due the urban washout (rainwater) that washes away drops of oil and sediments <sup>3</sup>.

### 2.2 Overview of the most common contaminated sites

In the last decades, in Europe, the industrial expansion, the uncontrolled production of hazardous substances and the disposal of large quantities of waste materials, have led to considerable environmental issues, with the deterioration of soil and groundwater quality <sup>4</sup>. The data collected on contaminated sites in Europe show that the total number of identified contaminated sites is 2.5 million, while the estimated number of potentially contaminated sites is 11.7 million <sup>3</sup>. The main problem is related to the contamination caused by municipal and industrial wastes (37%), followed by the industrial/commercial sector (33%). The storage (oils,

chemicals) contributes to 10.5%, while nuclear operations contribute only to 0.1% <sup>4</sup>. Concerning the soil contamination, mineral oil and heavy metals are the main contaminants contributing with a percentage equal to 60% <sup>3</sup>. The distribution of sectors contributing to soil contamination in Europe (with special focus to industrial and commercial activities) is shown in Figure 1 <sup>3</sup>.

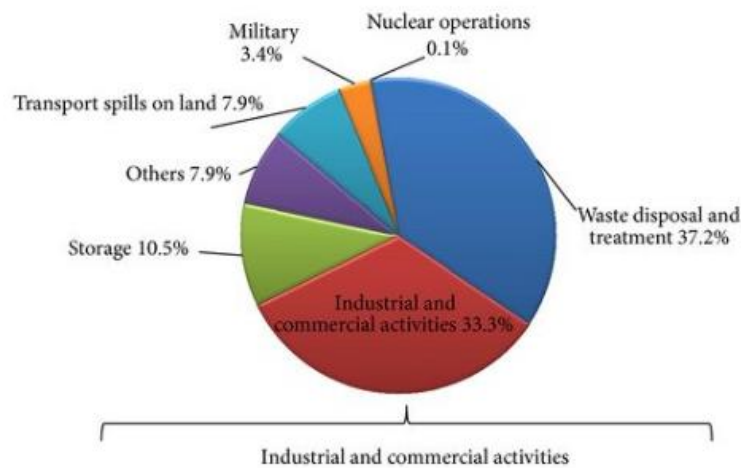


Figure 1 - Sectors contributing to soil contamination in Europe (Journal of Environmental and Public Health, 2013)

In order to evaluate how pollution could affect the environment, an overview on contaminants affecting soil and groundwater is necessary (Figure 2) <sup>3</sup>.

The contamination effects depend on the different properties of the contaminants such as diffusion, solubility in water and bioavailability <sup>4</sup>. After being released in the environment, they can migrate from the source of contamination, reach the groundwater and due to the groundwater flow the contamination can be transported and reach the receptors.

The main contaminant categories are mineral oil and heavy metals for both solid and liquid matrices, compared with the contribution of phenols and cyanides that can be neglected <sup>5</sup>. Heavy metals are considered dangerous due to their persistence and toxicity, but their concentration depends on the materials and soil properties. Major sources include industrial activities as mining activities, refineries or fossil fuels use. In groundwater, chlorinated hydrocarbons (CHC) have a greater contribution on soil contamination as well as aromatic hydrocarbons like benzene, toluene, ethylbenzene, xylenes (BTEX) <sup>5</sup> that occur naturally in crude oil.

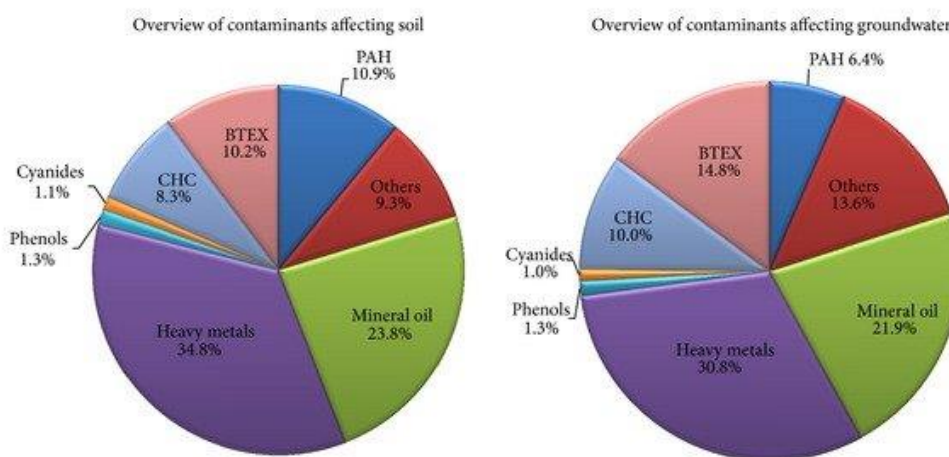


Figure 2 - Distribution of contaminants affecting soil and groundwater in Europe (Journal of Environmental and Public Health, 2013)

The European Environment Agency (EEA) defines the CHCs as chemicals containing the elements carbon and hydrogen, where one or more hydrogen atoms are replaced by chlorine atoms. The large use of this group of contaminants is related to the industrial sector as solvents and in agriculture as pesticides. In particular, the term can be used to describe the Persistent Organic Pollutants (POPs). POPs are persistent into the environment due to their high resistance to chemical degradation and their damage is mainly related to their diffusion in water and soil. Among POPs there are different recognized classes: chlorinated solvents, organochlorine pesticides such as dichloro-diphenyl-trichloroethane (DDT) and industrial chemicals such as polychlorinated biphenyls (PCB) and other organic compounds <sup>6</sup>.

Among chlorinated solvents, chloroethenes are the most common contaminants detected in groundwater systems. They are volatile organic compounds (VOCs) that consist of two carbon atoms joined by a double bond with the presence of chlorine atoms <sup>7</sup>. Chlorinated compounds are used in industrial, agricultural and commercial sectors and their large use led to an important diffusion of contamination <sup>8</sup>. Tetrachloroethene (PCE), trichloroethene (TCE), dichloroethenes (DCEs) and vinyl chloride (VC) can be found in the environment as result of past disposals of liquid and solid wastes on the ground or due to accidental spills into soils and groundwaters during handling and transportation <sup>9</sup>.

PCE (Figure 3) is mainly used as solvent for dry-cleaning, textile processing and as degreasing agent for military and industrial applications. It is a colorless, volatile and nonflammable liquid that is known to have toxic effects on human health. The effects are related to the nervous and

reproductive systems, irritation of the respiratory tract and eyes and kidney disfunction <sup>10</sup>. The compound is characterized by the ability to dissolve fats, greases and oil and by low solubility in water. Low solubility leads to unfavorable conditions in term of degradation in aquifers, low attenuation capacity and high persistence, causing long residence time in groundwater for decades.

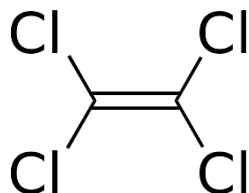


Figure 3 - Structure of PCE (wikipedia.org)

TCE (Figure 4), as PCE, is a nonflammable colorless liquid that is used as a dry-cleaning agent and metal decreasing solvent. Because of its moderate water solubility, TCE in soil has the potential to migrate into groundwater. The relatively frequent detection of TCE in groundwater confirms its mobility in soils. According to its occurrence in drinking-water supply relying on contaminated groundwater, it is necessary to study the risk attributed to human health. The main effects related to TCE are cancer and congenital heart effects <sup>11</sup>. The exposure primarily takes place in industries that use these kinds of chemicals (many dry-cleaning facilities) and in the industries that manufacturing chemicals or by the assumption of contaminated water. In order to manage the exposure, the industries undertake to check the contaminant levels in the humans measuring TCE or PCE concentrations in the blood and urine <sup>12</sup>.

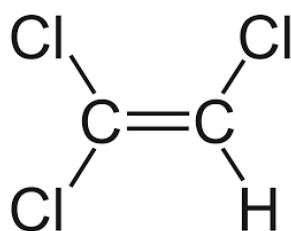


Figure 4 - Structure of TCE (wikipedia.org)

Both PCE and TCE, being VOC, are widely dispersed in atmosphere and transported for long distances in the air. Once they enter the environment, they can persist into the subsurface for many years due to their chemical stability and low solubility in water <sup>7</sup>. Typically, they are

released to surface water and land, and can be detected in drinking water supplies from groundwater sources. Moreover, they are common dense nonaqueous phase liquid (DNAPL) and having a density higher than water, they can migrate through the subsurface, reach the aquifer and penetrate deeply into the saturated area<sup>13</sup>. TCE and PCE, as a result of spilling, can be found as a free product, as a residual saturation into the saturated zone, as dissolved molecules into the subsurface and as absorbed fraction on the soil<sup>14</sup>. Once reached the aquifer, their migration will depend on different processes including biodegradation. The biodegradation (i.e. biotic breakdown) of PCE and TCE allows to obtain degradation products as DCEs and VC. Particularly, biodegradation in the long term may cause a complete dechlorination, transforming the compounds in not toxic final products.

The spreading into the unsaturated zone and atmosphere is caused by their high volatility<sup>15</sup>. In detail, DCE is a highly flammable, colorless liquid with a harsh odor. It is typically used to produce solvents and in chemical mixtures. Due to its high vapor pressure and low water solubility, it is possible to find high concentrations in atmosphere. Being a chlorinated solvent, the exposure is related to inhalation and due to its low relative molecular mass and hydrophobic nature, dermal absorption is also considered an exposure way. Following the inhalation exposure, the liver and the kidney are the principal target organs. In groundwater, biotransformation of DCE can form VC through reductive dechlorination<sup>16</sup>. The World Health Organization provides information about VC. It is a chlorinated hydrocarbon occurring as a colorless, highly flammable gas with a sweet odor. It is heavier than air and it has relatively low solubility. Because of its solubility in water, VC can be transported through the soil to groundwater. Typically, it is used for the manufacturing of plastic to produce polyvinyl chloride (PVC). For this reason and considering also its high vapor pressure, it has been found in the air near processing plants or hazardous waste sites. Exposure to high levels in the air can mostly affect liver and the central nervous system. It is considered as a human carcinogen.

When chlorinated solvents meet clay layers in their downward passage, they may pool on top of the clay, or seek a downward passage around the clay layer accumulating over time. Due to the low permeability of these layers, the migration occurs by dissolution and diffusion. With groundwater flow moving through permeable layers (sand, gravel) and encountering such secondary sources in the subsurface environment, the chlorinated solvents slowly dissolve into the groundwater up to their solubility limits. As groundwater moves, the contaminant will move with the contaminated water, slower due to delay phenomena, creating contaminated plumes<sup>7</sup> (Figure 5).

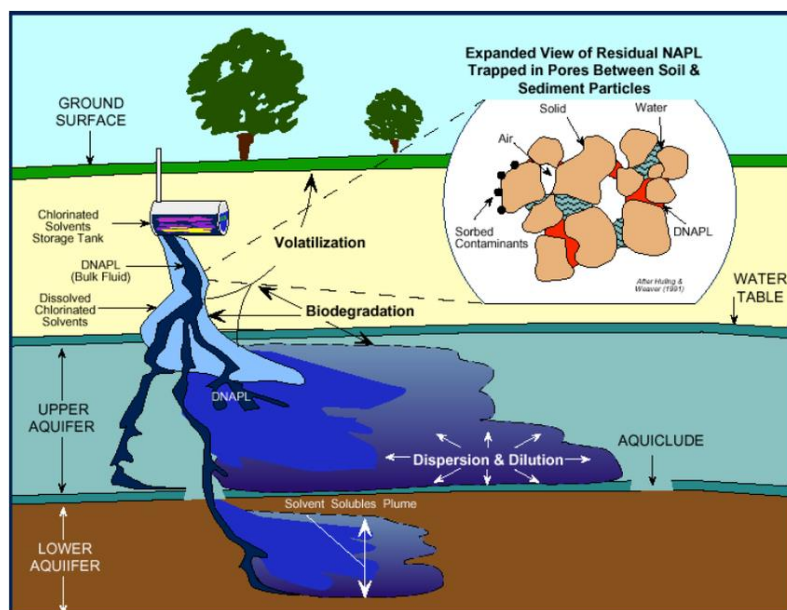


Figure 5 - Schematic of chlorinated solvent pollution migrating downward in an aquifer (U.S. EPA 1999)

Organochlorines pesticides (OCPs) have been used in large quantities in order to destroy insects or pathogens, resulting in large amounts of soil residues and groundwater. These chemicals are characterized by high toxicity and persistence, slow degradation, bioaccumulation and long-range transport<sup>17</sup>. Typically, they are defined as lipophilic because of their tendency to accumulate in fat tissues. DDT is a colorless solid, very soluble in fats and organic solvents and insoluble in water. It is persistent in the environment and the degradation and biodegradation processes occur slowly. Due to its low cost it has been used mostly as insecticide in developing countries of Asia, in order to control insects in crop production that may spread malaria and typhus. It was proved to have carcinogenic effects and was banned, under the Stockholm Convention in 2001, for all uses except for malaria control<sup>18</sup>.

PCBs (Figure 6) are a group of man-made organic chemicals whose properties depends on the number of chlorine atoms. Moreover, according to the position of chlorine atoms in the benzene ring, there are 209 kinds of different congeners<sup>19</sup>. They are typically used as lubricants in electrical equipment and as coolants, due to their heat and chemical stability<sup>20</sup>. Once PCBs are released into the environment they can accumulate in sediments and soils and persist with half-lives of months to years. Their environmental fate depend on their environmental mobility and they can be found at great distances from where they were released<sup>21</sup>. In particular, the transport is driven by different processes such as volatilization, partitioning, chemical or biological transformation and bioaccumulation. Their physical properties vary based on their class, but in general PCBs are small molecules with a low solubility in water and because of their

lipophilicity, they can be found in fatty tissues. The population can be exposed to PCBs through contaminated food ingestion or inhalation. These compounds have low acute toxicity. However, chronic toxicity represents serious health problems mainly related to the skin and liver damage <sup>19</sup> and may affect the reproductive system or damaging the immune and nervous system <sup>20</sup>.

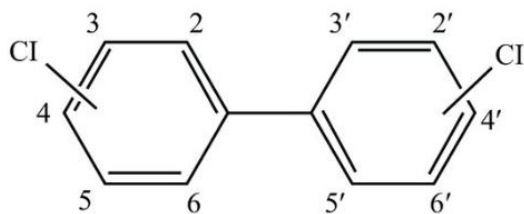


Figure 6 - Structure of PCBs (researchgate.net)

BTEX are another class of chemicals which is part of VOCs. Typically, these compounds are found in petroleum products and due to leakage from underground storage tanks or accidental spills, they are one of the most common contaminants present in soil and groundwater. Thanks to their polarity and very soluble characteristic, they are able to enter the soil and groundwater systems causing serious pollution problems <sup>22</sup>. For this reason, one of the most common way of exposure is drinking water, but exposure can also occur by inhalation of polluted air or from dermal contact. Due to this, the effects of BTEX are related to skin irritation, nervous and respiratory system problems <sup>22</sup>.

### 2.3 In situ chemical oxidation

The initial remediation approach for the contaminants described above was related to physical remediations, involved using pumping wells to extract contaminated groundwater, followed by treatment of the extraction of groundwater (pump and treat). Due to the hydrological systems complexity, these kinds of treatments are considered slow and inefficient <sup>23</sup>. Therefore innovative remediation technologies have been developed including in situ chemical oxidation (ISCO) <sup>7</sup>.

ISCO technology is based on the principle of redox reactions that involve a transfer of electrons between two species: the reagent, an oxidant agent that is reduced and the reducing agent, the contaminants that are oxidized. With the application of ISCO a reactive zone is created by the introduction of strong chemical oxidants that are injected into the subsurface with different methodologies <sup>24</sup>. In this way the contaminant is completely mineralized or transformed in a less toxic and harmful product.

The efficiency of the process depends on the properties of the used oxidant, its capability to degrade organic compounds and the subsurface conditions<sup>24</sup>. In this regard, to have a successful result, the distribution technique should ensure that the oxidant distribution is uniform in the entire treated area<sup>25</sup>. The oxidant injection includes different delivery methods. Particularly, two approaches are described and shown in Figure 7:

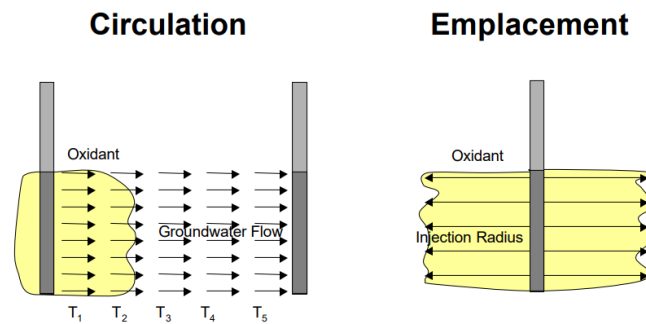


Figure 7 - Delivery approaches

1. Direct emplacement: it is based on the fast injection of the oxidant solution in the area to be treated. This method is typically used for sites that provide a rapid oxidant decomposition and a shorter injection spacing;
2. Circulation: it is a method in which a modified groundwater flow pattern is used to control the distribution of the contaminant in the area that need to be treated, combining injection and groundwater extraction: the oxidant is injected into one well and the groundwater with the oxidant is pumped out in another well (Figure 8)<sup>25</sup>. It is used for sites that show high half-live (>20h)<sup>26</sup>. The wells are usually installed at different depths, in order to reach as much dissolved and undissolved contaminants as possible (Figure 9)<sup>25</sup>.

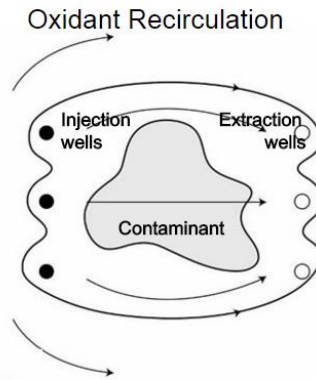


Figure 8 - Recirculation method used in ISCO (Interstate Technology and Regulatory Council, 2005)

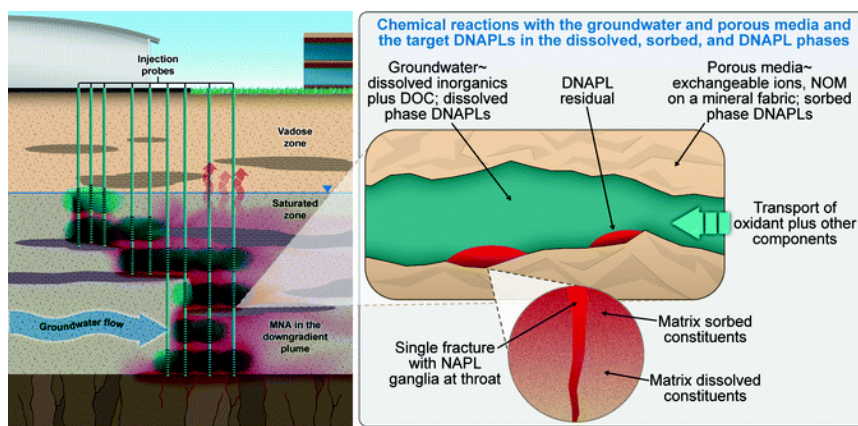


Figure 9 - ISCO using direct-push injection probes (ISCO for groundwater remediation, Siegrist et al (2011))

To be effective, ISCO technologies require a detailed level of understanding based on:

- **the site characteristics:** site history, location of contaminant release, geology and hydrology;
- **the subsurface biogeochemistry:** redox potential, reactivity of the subsurface with the selected oxidant, pH and alkalinity and presence of redox-sensitive metals.

### 2.3.1 ISCO reactants

ISCO treatment includes different oxidants such as sodium or potassium permanganate, hydrogen peroxide (Fenton's reagent), ozone and recently peroxydisulfate (PDS) <sup>7</sup>.

#### Permanganate

Permanganate is one of the most common oxidants used in ISCO. It is applied for the oxidation of different organic compounds, with a focus on chlorinated solvents, hydrocarbon compounds and other organic compounds in soil and groundwater. The permanganate ion is a transition

metal oxidant with a high reduction potential of 1.68 volts (V) at acidic pH and derives its oxidizing power from manganese in the heptavalent form (Mn[VII])<sup>27</sup>. There are two forms of permanganate that are used in ISCO applications: sodium permanganate (NaMnO<sub>4</sub>) and potassium permanganate (KMnO<sub>4</sub>). Concerning the process, they have the same oxidation chemistry, but there are some differences related to the impact on design of ISCO system. Sodium permanganate can be directly mixed in water and this property ensures that the oxidant is delivered directly to the interested site<sup>27</sup>. Typically, ISCO using sodium permanganate involve the following steps:

1. Installation of injection wells and associated equipment;
2. Preparation of a dilute reagent solution from a concentrated NaMnO<sub>4</sub> solution;
3. Injection of the reagent solution.

The injection can occur through a high pressure direct-push technology.

The main characteristics of sodium permanganate are related to its capability to react in a wide range of pH and to its chemical stability; this is the reason why it is the most used oxidant in environmental applications<sup>28</sup>. A problem related with potassium permanganate is the oxidant precipitation that can occur in the subsurface. Since the temperature in the aquifer is less than the temperature of the place in which the oxidant is mixed, when high concentrations are used and they react with temperatures higher than groundwater's, it can precipitate forming a solid compound that does not easily react with the contaminants, due to the strong dependence between temperature and solubility<sup>29</sup>. This may cause temporary well plugging in some situations, especially in lower hydraulic conductivity media as the precipitates may aggregate<sup>24</sup>. When permanganate is injected into the subsoil it readily reacts with organic matter and reduced species. The total amount of permanganate necessary to satisfy the consumption of the oxidant by groundwater and soil is known as natural oxidant demand (NOD) and it can limit the effectiveness of ISCO. Using permanganate, the natural organic matter (NOM) competes with the target compounds and permanganate concentration available for the degradation of contaminants decreases due to the oxidation of dissolved organic compounds. It is necessary to monitor this parameter, in order to understand the amount of permanganate available for the destruction of contaminants as well as the dispersion and persistence of permanganate in the subsurface<sup>30</sup>.

Huang et al. (2000) formulated an equation in order to evaluate NOD of a soil, using potassium permanganate<sup>31</sup>:

$$\text{NOD} = \frac{V([\text{KMnO}_4]_0 - [\text{KMnO}_4]_f)}{m_{\text{soil}}}$$

where,

- *NOD* is natural oxidant demand (g/kg);
- *V* is total slurry volume (L);
- $[\text{KMnO}_4]_0$  is initial potassium permanganate concentration (g/L);
- $[\text{KMnO}_4]_f$  is final potassium permanganate concentration (g/L);
- $m_{\text{soil}}$  is mass of dry soil (kg).

The oxidation occurs with the electron transfer through the following reactions:



Eq.1 involves the transfer of five electrons and under acidic conditions, the reaction may become dominant and alter reaction mechanisms<sup>24</sup>. On the other hand, in Eq.2 three electrons are transferred. Eq.2 represents the most typical reaction that takes place at contaminated sites and allows the formation of manganese oxides. Alkaline permanganate oxidation (pH > 12) represented by Eq.3, is generally unlikely to occur in ISCO because this high pH value falls outside the normal range for groundwater environments<sup>24</sup>. In these reactions there is the manganese reduction from  $\text{Mn}^{+7}$  form to  $\text{Mn}^{+6}$ ,  $\text{Mn}^{+4}$ ,  $\text{Mn}^{+2}$  respectively<sup>32</sup>.

The production of manganese oxides leads to the formation of significant deposits in the subsurface and has an impact on the flow around permanganate injection area. Depending on the reaction, manganese oxides can be colloidal, particulate or in form of bulk matrix directly precipitated on the solid. The precipitation of manganese oxides has negative effects on both the oxidant distribution and the effective contact between the oxidant and the contaminants are the main characteristics of manganese oxides. Some studies have demonstrated that these particles are able to reduce the permeability by blocking pores<sup>33</sup>. The particles can also deposit between a DNAPL and the aqueous phase causing a loss in degradation efficiency. On the other hand, they result very effective against heavy metals: the solids produced can immobilize the metals such as cadmium, increasing the sorption potential of the aquifer sediments<sup>34</sup>.

### Fenton's reagent

Fenton's reagent is composed of hydrogen peroxide ( $H_2O_2$ ) and ferrous iron. The reagent in the liquid form is injected into the subsoil in order to oxidize organic compounds such as hydrocarbons, chlorinated solvents, polycyclic aromatic hydrocarbons (PAHs) and polychlorinated biphenyls (PCBs). The oxidation is driven by a radical mechanism that consists of the formation of radicals during the reaction between hydrogen peroxide and the catalyst (i.e. the ferrous iron)<sup>32</sup>. The term radical (or free radical) is referred to an atom, molecule or ion that has at least one unpaired electron in its outermost orbital. This is the reason why radicals are very active and are able to react with a several number of pollutants<sup>35</sup>. Typically, the catalyst applied is Fe (II) that reacts with hydrogen peroxide producing hydroxyl radicals and Fe (III) as shown in Eq.4:



The hydroxyl radicals are responsible for the oxidation of organic compounds cited above.

Fe (III) reacts again with the  $H_2O_2$  and produces perhydroxyl radicals:



The main disadvantage of Fe (III) is its limited solubility in water, for this reason it is necessary to decrease pH (2-3) in the subsurface. Another problem is related to the  $H_2O_2$  instability. Due to the reactions that take place within some soil or groundwater, there is a loss in  $H_2O_2$  concentration that lead to a reduction in the efficiency of Fenton's reaction<sup>32</sup>. If high concentrations of  $H_2O_2$  are used, with the aim to reduce residual concentrations of contaminants by volatilization, the reaction may be uncontrolled. In this way it can cause an excessive rise in temperature, vapors and possible explosions can occur, creating dangerous issues for the operators. Moreover, it results hard to handle because of its rapid oxidation. In this regard it would be necessary to dose it continuously<sup>28</sup>.

### Ozone

Ozone ( $E^0 = 2.07 V$ ) is characterized by a high oxidant capacity and for this reason it is used in ISCO applications, mainly for the degradation of PAHs and BTEX. Typically, as cited above for the other reagents, it is injected using vertical or horizontal wells and it induces the direct contaminants oxidation. Being a gas it can be applied for treating both the vadose zone and the saturated zone<sup>36</sup>. The oxidation of organic compounds by ozone takes place in two ways: by

direct oxidation with ozone molecules or by the generation of free-radical intermediates, like hydroxyl radical<sup>36</sup>. Ozone is not a stable molecule: due to its high reactivity and short life (20 min) it is necessary to produce the ozone close to the treatment area using oxygen or atmospheric air<sup>28</sup>. A secondary effect of ozone treatment is the generation of oxygen, which promotes the aerobic degradation of the hydrocarbons on a longer term.

### Peroxydisulfate

In the last years, PDS has been proposed for ISCO processes as an effective alternative to permanganate, due of his high stability and high reactivity with a several contaminants<sup>37</sup>. Use of PDS as an alternative oxidant has the potential to eliminate problems associated with manganese precipitation. However, PDS in combination with an activator leads to the formation of radicals able to form a more powerful oxidant able to degrade a wider range of contaminants at faster rates<sup>38</sup>. Sodium PDS is the most common salt used to treat contaminated soils<sup>32</sup>, since potassium PDS presents a low solubility, while the application of ammonium PDS could lead to the formation of ammonia.

## **2.4 Peroxydisulfate**

### **2.4.1 Mechanisms of PDS reactions**

PDS is a stable and strong oxidant with a high oxidation potential ( $E^0 = 2.1 \text{ V}$ ). In the direct oxidation two electrons are simultaneously transferred with low reaction rate (Eq.6):



Due to its symmetric structure and its high bonding energy, the separation of O-O bonds appears difficult and the reaction rates decrease with increasing number of bonds<sup>39</sup>. In specific conditions, in order to increase its reactivity with the contaminants, it can be activated to form radicals<sup>40</sup>. Because of PDS stability and its long half-life (600 days at 25 °C), it can be delivered at considerable distances in the subsurface, before being activated for contaminant degradation<sup>41</sup>. In order to generate sulfate radicals ( $\text{SO}_4^{\bullet-}$ ) and hydroxyl radicals ( $\bullet\text{OH}$ ), PDS can be activated by thermal, alkaline, UV radiation, ultrasound,  $\text{H}_2\text{O}_2$  and transition metals. Recent studies have demonstrated that sulfate radicals have some advantages compared with hydroxyl radicals, such as higher oxidation potential (2.5-3.1 V), higher selectivity and efficiency to degrade contaminants and wider pH range. For neutral pH, sulfate radicals present higher oxidation potential than hydroxyl radicals, however, it has been demonstrated that for acidic pH their behavior is similar<sup>42</sup> to hydroxyl radicals. On the other hand, hydroxyl radicals

exhibit a relevant redox potential of 2.8 V that permit to oxidize a considerable variety of organic compounds.

### Thermal activation

In order to increase the decomposition rate, the thermal activation can be used. This process needs temperatures between 35-130 °C. The rise of temperature accelerates radicals' production, solubility and degradation of organic pollutants. Furthermore, it is evident that this process is pH dependent. With pH values lower than 2, PDS decomposes without the formation of radicals <sup>43</sup> and at pH lower than 7 most pollutants cannot be completely removed <sup>42</sup>. High temperatures can permit the fission of O-O bond to form sulfate radicals (Eqs.7-8):



During the heat process, sulfate radicals are transformed into hydroxyl radicals, following Eq.9, with a slow reaction rate <sup>42</sup>:



The most common pollutants treated using thermal activation of PDS are the chlorinated organic solvents such TCE and trichloroethane (TCA), mostly applied in chemical, pharmaceutical and other industries <sup>28</sup>. The rise in temperature allows to reach a higher level of sulfate free radical production due to the rise in activation energy and then higher removal efficiency due to the high reaction velocity between chlorinated solvents and PDS. It is reported that the reaction of TCE with activated PDS at 20 °C is very slow and only 7.6% oxidation is observed in 10 h. With temperatures equal to 30-50 °C, the TCE removal rate significantly increases and the remediation time decreases (Figure 10) <sup>44</sup>.

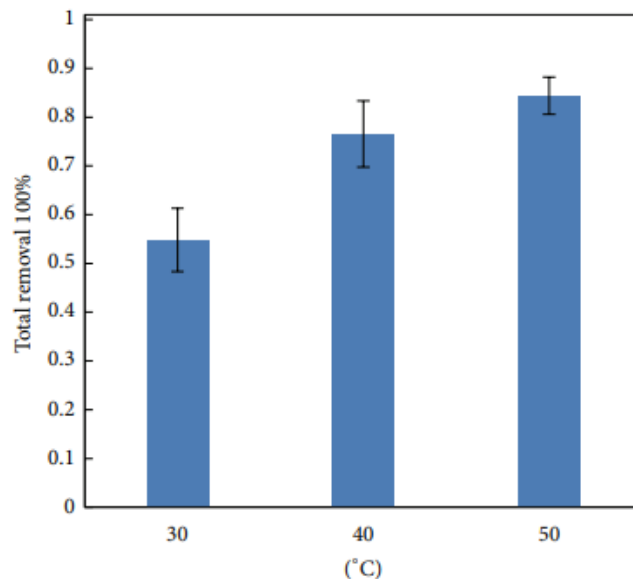


Figure 10 - The depletion of chlorinated organic solvents by activated PDS at different temperature 30 °C, 40 °C, 50 °C (Liu et al. (2014))

Thermal activation appears an effective mechanism for PAHs removal, toxic, persistent and carcinogenic compounds. The rise in temperature allows the rise of contaminant removal and redox potential values. When unactivated PDS is used, a small removal of the compounds occurs, but the activated PDS by thermal mechanisms leads to a removal of 87-99%<sup>45</sup>. It is necessary to consider that the oxidation rate of PAHs depends on the kind of free radicals that are formed during the activation process. The hydroxyl radicals are the mostly generated during the thermal activation. Therefore, an increase in PAHs degradation is evident<sup>45</sup>.

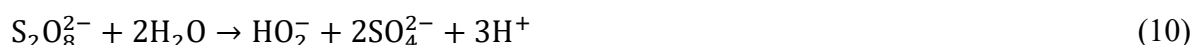
### Ultrasound activation

Ultrasound activation of PDS is an alternative method to degrade various organic compounds. It can occur in two ways. For both mechanisms the activation begins with induction of cavitation bubbles in a water solution. The first mechanism provides the collapse of the bubbles that leads to the generation of a hot spot characterized by high temperature (5000 K) and high pressure (1000 atm). In the second mechanism the cavitation bubbles lead to the generation of hydroxyl radicals due to the dissociation of water molecules<sup>46</sup>. The transformation of PDS to sulfate radicals depends on the increase of ultrasonic amplitude that allows to increase the cavitation effect<sup>42</sup>. The combination of PDS with ultrasound appears a great removal method for hydrocarbons in contaminated soils due to the raise of the contaminant desorption rate and mass transfer in the subsurface. The rise in PDS concentrations accelerates the reaction rate of chlorinated solvents due to the presence of higher concentrations of sulfate radicals, increasing

the dissolution and the desorption of contaminants <sup>47</sup>. The degradation efficiency increases significantly with the rise in ultrasonic power. With a high ultrasonic power, more cavitation bubbles are generated and more energy for radical formation is available. Generally, the ultrasonic power required is around 200 W. For the degradation of hydrocarbons, in order to increase the efficiency, acidic pH is preferred. In these conditions there is more production of sulfate free radicals <sup>48</sup>.

### Alkaline activation

Alkaline activation is the process that depends on the decomposition of PDS due to the presence of high pH and it is considered an efficient approach due to the fast decomposition of PDS under alkaline conditions <sup>43</sup>. The mechanism takes place when PDS is mixed with KOH or NaOH to raise the pH between 11 and 12. This mechanism is utilized in order to allow the radicals' formation and the transformation of sulfate radicals in hydroxyl radicals. The mechanism involves the hydrolysis of PDS to hydroperoxide anion ( $\text{HO}_2^-$ ) and sulfate ( $\text{SO}_4^{2-}$ ) (Eq.10):



The hydroperoxide formed from the hydrolysis of one PDS molecule reduces another PDS molecule, generating sulfate radical and sulfate anion (Eq.11):



In highly alkaline conditions, sulfate radical reacts with hydroxide to form hydroxyl radical ( $\text{OH}^\bullet$ ) (Eq.12):



Hydroxyl radicals are the dominant reactive species at  $\text{pH} > 12$ , resulting in a several number of contaminants degradation <sup>49</sup>.

As an example, the alkaline activation has been applied in the case of dichloromethane (DCM), a chlorinated VOC found in contaminated soils, air and groundwater due to its large use as solvent in chemical industry. The main characteristic of DCM is its high volatility and resistance to degradation. Once alkali (NaOH) is used to activate PDS, there is the formation of sulfate and hydroxyl radicals, with the predominance in hydroxyl radicals' production, able to degrade DCM. The rise in oxidant concentration leads to a rise in degradation rate of the pollutant and when the  $\text{pH} > 12$  is reached, the degradation is no more affected by the molar ratio between NaOH and PDS <sup>50</sup>.

### Activation using H<sub>2</sub>O<sub>2</sub>

PDS can be used in combination with H<sub>2</sub>O<sub>2</sub> in order to allow the activation. It is a common technology applied with the aim to remove chlorinated ethenes, dichloromethane and BTEX<sup>43</sup>. Typically, it is directly injected into the subsurface along with PDS and once in the subsurface the hydrogen peroxide reacts with the soil compounds producing a decomposition reaction<sup>51</sup> and leading to the formation of hydroxyl radicals (Eq.13)<sup>43</sup>:



H<sub>2</sub>O<sub>2</sub> as short half-life and in practical applications tends to rapidly decompose. In order to have successful outcome, multiple injections of hydrogen peroxide are required<sup>51</sup>.

### Ultraviolet activation

Ultraviolet (UV) activation is used to produce sulfate radicals for the destruction of organic compounds. Among radiation activation methods is important to mention also gamma ray and ultrasonic, but UV radiation is considered the most common way to activate PDS due to its low cost and high capacity for removing organic compounds from groundwater<sup>42</sup>. The process is driven by the reaction shown in Eq.14:



The UV energy breaks the O-O bond similar to heat-activated PDS<sup>49</sup>. In this kind of process, it is necessary to consider an important parameter, the quantum yield, i.e. the ratio of the number of photons emitted to the number absorbed. Once UV wavelength increases, quantum yields decrease and a decline in sulfate radicals' formation is evident. The UV light radiation plays an important role in PDS activation and organics degradation. The most common wavelength value utilized is 254 nm<sup>42</sup>, due to lower reaction time needed compared with the other wavelengths<sup>49</sup>.

Phenol is one of the pollutants that can be removed using PDS activated by UV radiation. Phenols are commonly present in aqueous phases due to its large use in petrochemicals, textiles and pharmaceuticals industries. Using UV light, the degradation rate constant of phenol increases with increased PDS concentration. On the other hand, oxidation rate efficiency decreases as initial phenol concentration increases. Considering the wavelength value of 254 nm, the phenol has a high absorption capacity. Therefore, the rise in phenol concentrations makes the solution impermeable to UV radiation<sup>52</sup>.

### Activation using transition metals

Activation based on transition metals is the most commonly used PDS activation technology. Transition metals and metal oxides are commonly used due to non-toxic characteristics, low costs and low complexity in the application<sup>35</sup>. Among the metal catalysts, iron and its oxides are the most used. They are environmentally friendly, non-toxic and more cost effective than other transition metals. Their application provides an efficient contaminant decrease and a significant activation efficiency<sup>37</sup>. The sulfate radical formation occurs according to the free radical formation mechanism. The transition metal, such as iron, reacts with PDS as shown in Eq.15:



through the two steps:



The production of sulfate radicals takes place when  $\text{Fe}^{2+}$  is converted in  $\text{Fe}^{3+}$  (Eq. 17), but it is necessary to find the right molar ratio between PDS and iron, in order to allow the reaction to take place. Too much  $\text{Fe}^{2+}$  results in the iron scavenging of the sulfate radicals.

The main problem is that for  $\text{SO}_4^{\bullet-}$  there is competition between target organic contaminant and  $\text{Fe}^{2+}$  excess. Increasing in  $\text{Fe}^{2+}$  concentrations lead to a rise in reaction velocity (Eqs.16-17) that can destroy  $\text{SO}_4^{\bullet-}$ , decreasing the degradation efficiency of the contaminant target<sup>32</sup>.

In order to optimize the oxidation and increase PDS decomposition, it is necessary to decrease the reaction velocity partially adding  $\text{Fe}^{2+}$  into the environment<sup>32</sup>. Moreover, to maintain the iron in solution, different chelating agents are used. The citric acid (CA) effectively control the  $\text{Fe}^{2+}$  precipitation, it is environmentally friendly, readily biodegradable and can extract toxic metals from contaminated soils. Ethylenediamine tetraacetate (EDTA) is the most used chelating agent, due to its strong complexes with iron ion. It can slow-down the  $\text{SO}_4^{\bullet-}$  production and prevent  $\text{SO}_4^{\bullet-}$  scavenging due to the excess of  $\text{Fe}^{2+}$ <sup>53</sup>. Examples of iron activated PDS treatment include BTEX/phenols, pharmaceuticals and various other organics.  $\text{Fe}^0$  is thought to act with PDS slower than  $\text{Fe}^{2+}$ , increasing the ability to activate PDS<sup>49</sup>.  $\text{Fe}^{3+}$  may also activate persulfate but may be less reactive or, under certain conditions, may be converted to  $\text{Fe}^{2+}$ <sup>54</sup>.

A typical example of this mechanism is the degradation of phenol using the system  $\text{Fe}^{2+}$ -PDS. To increase the degradation efficiency, CA and trisodium citrate (TC) are used. The release of  $\text{Fe}^{2+}$  in the solution is slow and a delay in  $\text{SO}_4^{\bullet-}$  formation is evident. The simple system  $\text{Fe}^{2+}$ -PDS has less effectiveness than  $\text{Fe}^{2+}$ -CA/PDS and the removal of phenol is significantly improved using this kind of system. In contrast, a high TC concentration leads to an inhibition in phenol due to the degradation of excess citrate. According to Maoying Fang et al. (2019) the optimum conditions to operate are related to the PDS concentration of 0.06 mol/L, a  $\text{Fe}^{2+}$  concentration of 0.02 mol/L and TC concentration of 0.01 mol/L. Moreover, a temperature value of 35 °C is required in order to allow phenol removal <sup>55</sup>.

In groundwater remediation, TCE removal was investigated using PDS activated by CA-chelated- $\text{Fe}^{2+}$ . Experimental results showed that in presence of PDS almost the total amount of TCE can be removed. In particular, the efficiency of the process results higher thanks to the activation of PDS by using  $\text{Fe}^{2+}$ , that lead to the formation of free radicals able to react with TCE and similar compounds. In laboratory, Xiaoliang Wu et. al (2014) observed that the faster degradation occurred in presence of CA. During the first 30 s and once PDS was added into the system, due to the fast formation of free radicals, there was a fast oxidation of  $\text{Fe}^{2+}$  in  $\text{Fe}^{3+}$ . Then the compound was slowly degraded due to the accumulation of  $\text{Fe}^{3+}$  <sup>56</sup>.

Haizhou Liu et al (2014) examined the stability of PDS in presence of BTEX. The rate of PDS decomposition was increasing when benzene concentration was increasing. Moreover, in absence of benzene the half-life of PDS decreases from 170 days to 45-20 days in presence of 100-1000  $\mu\text{M}$  of benzene <sup>57</sup>.

Among BTEX compounds, benzene exhibits the higher resistance to PDS oxidation. Huang et al. (2005) demonstrated that VOCs with higher degradation rates in the presence of PDS, generally are characterized by C-C double bonds or are aromatic ring compounds with functional groups. The oxidation of BTEX occurs with higher efficiency in the case of higher solubility in water <sup>58</sup>.

#### **2.4.2 Free radical scavengers affecting peroxydisulfate oxidation**

The radical formation due to the activation of PDS, using different methods, leads to rapid reactions with the contaminants present in the subsurface, causing their degradation. However, the radicals are also able to react with non-target species that are present in solution. These reactions contribute to radical scavenging that typically causes treatment inefficiency and ineffectiveness <sup>27</sup>. The commonly radical scavengers present in groundwater are

carbonate/bicarbonate and chloride. Some experiments showed that their impacts are related to the inhibition of contaminant degradation, formation of free radicals and consume of PDS <sup>27</sup>, but others have shown that their reaction with other radicals allows to reduce rates of contaminant degradation <sup>27</sup>.

Carbonate and bicarbonate have the potential to affect PDS efficiency <sup>27</sup> and to react with Fe<sup>2+</sup> to form precipitates and interfere with production of SO<sub>4</sub><sup>•-</sup>, acting as metal complexing agents <sup>59</sup>. The adverse impact of carbonate on PDS is strongly related to pH, the rise in pH leads to a decrease in degradation rates <sup>60</sup>. Liang et al (2006), demonstrated the influences of carbonate on PDS oxidation of TCE in the laboratory experiments. In the case of neutral pH, the oxidation of TCE was not affected by the presence of carbonate/bicarbonate with a concentration between 0-9.20 mM. On the other hand, the scavenging reactions were evident in the case of elevated level of pH <sup>61</sup>. In addition, carbonate and bicarbonate can also form radicals that react with sulfate and hydroxyl radicals (Eqs. 18-19) <sup>27</sup>:



These radicals can be able to activate PDS and be productive in case of contaminant degradation <sup>60</sup>.

Chloride ion is the second radical scavenger that has the potential to affect oxidation efficiency. For example, in the case of heat activated PDS, the degradation efficiency decreases when concentrations of chloride are more than 20 mM at 130 °C. Moreover, high concentrations of chloride (>100 mM) can lead to the formation of halogenated by-products, during the treatment of PCE using PDS <sup>60</sup>. This formation usually takes place at sites with high chloride concentrations. Chloride is known because of its reaction with other radicals, such as sulfate and hydroxyl radicals (Eqs. 20-21) <sup>27</sup>:



Sulfate radicals are more sensitive to the presence of chloride, since the reaction between them is pH dependent. Chloride radicals may participate to the removal of organic contaminants by activating PDS but on the other hand high concentrations may cause scavenging of sulfate and

hydroxyl radicals decreasing efficiency of oxidation process <sup>62</sup>. Chloride radical (Cl•) can react with the contaminants producing toxic by-products such as chloroethanes <sup>63</sup>.

### 2.4.3 Persistence of unactivated PDS in the presence of aquifer solids

The persistence and the stability of the oxidant give information about its mobility in specific subsurface zones. Persistence describes how long the oxidant will last and its evaluation is based on the information about PDS decomposition rates <sup>64</sup> and on the interactions between PDS and soil oxidizable matter (SOM) <sup>37</sup>.

The persistence of unactivated PDS in the presence of aquifer materials is evaluated using the kinetic approach or the soil oxidant demand (SOD) concept. In the kinetic approach the data are referred to PDS concentration in function of time and the reaction order and rate constant are determined <sup>39</sup>. On the other hand, SOD is referred to the oxidant concentration that is consumed in non-target reactions with contaminants and natural agents. It is expressed in grams of PDS consumed per kilograms of soil <sup>65</sup>.

In order to study PDS decomposition by a kinetic point of view, some studies explained that the decomposition follows a first-order rate law. A first-order reaction is a reaction that proceeds at a rate that depends linearly on only one reactant concentration. The rate law for the decomposition of PDS is:

$$\frac{d [S_2O_8^{2-}]}{dt} = -k_{obs}[S_2O_8^{2-}] \quad (22)$$

where  $k_{obs}$  is the first-order reaction rate coefficient (in units of 1/time).

In order to understand if the reaction in question is respecting the first-order law, it is necessary to plot the natural logarithm of the concentration versus time. The result will give a straight line with the slope of the line equal to -k. Particularly, the behavior of the reaction will be evident plotting the concentration versus time, obtaining an exponential curve indicating the first-order rate law <sup>66</sup> (Figure 11).

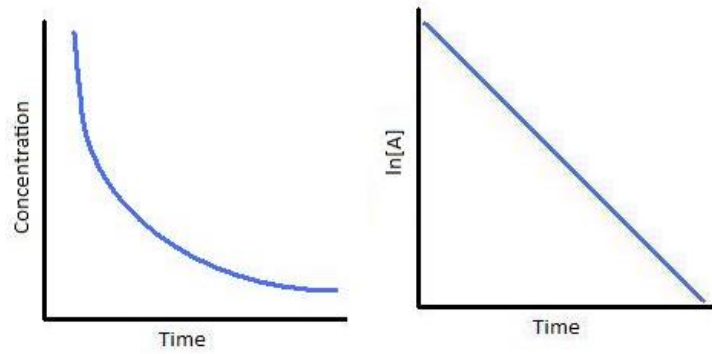


Figure 11 - Concentration of reactants vs time for a first-order reaction

Moreover, knowing the reaction rate coefficient, will be possible to calculate the half-life ( $t_{1/2}$ ), related to the amount of time needed for a reactant concentration to decrease by half compared to its initial concentration. The half-life for first-order reaction is independent on the initial concentration of reactant and it is calculated as:

$$t_{1/2} = \frac{\ln 2}{k}$$

In this purpose, knowing  $k$  and  $t_{1/2}$ , it will be possible to describe PDS persistence and decomposition velocity in time <sup>66</sup>.

The processes that are related to the transport of the oxidant are time dependent. If the transport of the oxidant covers short distances, contact time is limited and the contaminants degradation is ineffective <sup>39</sup>. On the other hand, the oxidant must persist long enough in order to obtain a remarkable contaminant degradation <sup>27</sup>.

The reaction rate depends on different factors related on the ionic strength, on iron content (Fe) and on total organic carbon (TOC) content <sup>67</sup>.

The ionic strength represents a measure of the concentration of ions in a solution and it is controlled by the initial concentration of PDS. The ionic strength is calculated as the sum of the molar concentration of each ion multiplied by the valence squared:

$$I = \frac{1}{2} \sum_{i=1}^n c_i Z_i^2 \quad (23)$$

where,

- $c$  is the molar concentration (mol/l);
- $z$  is valence for each ion.

When PDS is decomposed in sulfate ( $\text{SO}_4^{2-}$ ) and proton ( $\text{H}^+$ ), the ionic strength rises, and its rise leads to the increase of degradation of organic compounds. The PDS stability is proportional to ionic strength, but the most relevant parameters related to the stability are TOC and Fe. Estimating the sum of specific reductive species, the total reductive capacity of an aquifer material can be theoretically determined. In order to quantify it from an experimental point of view, the chemical oxidant demand (COD) is evaluated.

TOC is the measure of the level of organic molecules or contaminants in purified water and basically represents the natural organic matter (NOM) content <sup>67</sup>.

The interactions of PDS with the porous medium have a considerable importance in term of injection and effectiveness of the oxidant in the subsurface <sup>39</sup>. When the oxidant is injected into the subsurface it is consumed also by the non-specific interactions with porous medium <sup>27</sup>.

In these conditions, with a rise in injected PDS concentrations an increase in PDS degradation is expected, which permits the transport of PDS away from the injection point through advection, diffusion and dispersion, in order to cover the entire treatment area <sup>67</sup>. PDS transport can be approximated with the one-dimensional advection-dispersion reaction equation (Eq.24) <sup>39</sup>:

$$\frac{\partial C}{\partial t} = D \frac{\partial^2 C}{\partial x^2} - v \frac{\partial C}{\partial x} - \lambda C \quad (24)$$

where,

- $C$  is PDS concentration;
- $t$  is time;
- $D$  is the dispersion coefficient;
- $x$  is a distance;
- $v$  pore velocity
- $\lambda$  is the rate of PDS decomposition.

The coefficient  $\lambda$  represents the natural degradation coefficient, related to the solutes subjected to natural degradation.

This coefficient depends on the half-life following the relation:

$$\lambda = \frac{\ln 2}{t_{1/2}}$$

In this way by understanding the decomposition kinetics, it is possible to design ISCO system in order to determine the distances with which PDS can be transported and injection rates <sup>39</sup>. Considering the case of solutes subjected to a natural degradation, the analytical solution of Eq.24 was obtained by Bear <sup>28</sup> (Eq.25):

$$\begin{aligned} \frac{C(x, t)}{C_0} = & \frac{1}{2} \exp \left[ \frac{v_e x}{2D_x} (1 - U) \right] \operatorname{erfc} \left( \frac{x - Uv_e t}{2\sqrt{D_x t}} \right) \\ & + \frac{1}{2} \exp \left[ \frac{v_e x}{2D_x} (1 + U) \right] \operatorname{erfc} \left( \frac{x + Uv_e t}{2\sqrt{D_x t}} \right) \end{aligned} \quad (25)$$

where,

$$U = \sqrt{1 + \frac{4\lambda D_x}{v_e^2}}$$

The decomposition rate of PDS is proportional to the oxidant concentration and to the soil oxidizable matter (SOM) <sup>67</sup>. Considering that SOM is the dominant factor that influence PDS decomposition, the analysis of SOM will be helpful for the determination of SOD <sup>37</sup>. The most contributors to SOD are the inorganic soil constituents and the naturally occurring organic material (NOM) <sup>68</sup>.

Persulfate has a low SOD versus permanganate, with values typically ranging from 0.05 to 5 g / kg, depending on soil type. SOD values in the case permanganate range around values of 0.4 and 240 g/kg. The relatively low SOD for persulfate may be a result of the fact that persulfate oxidation of SOM is an incomplete process, degrading the soil organics only 20 – 40% <sup>68</sup>.

Inorganics (such as Fe and Mn) can lead to the loss in PDS concentration due to the high reactivity with these components and its decomposition. This phenomenon is explained as a result of interactions between PDS and elemental components of the soil: if soil rich in Fe and Mn content, the half-life will be characterized by significant low values <sup>37</sup>.

Once PDS is injected into the subsoil, NOM reacts with the oxidant and a decay in PDS concentration will be evident. Consequently, with the rise in NOM the PDS demand will increase and remediation efficiency by PDS will be controlled by NOM <sup>37</sup>.

In soil, the removal rates of contaminants are lower because SOM competes with target contaminants for PDS <sup>39</sup>. Once SOM is removed the most responsible factors for PDS decomposition will be Fe/Mn-oxides. In the case of sandy soil systems, using PDS, the oxidant concentration will persist in soil due to the high content of Si that does not affect the rate of PDS loss, but this factor will depend on organic content that as explained above has a significant effect on PDS consume <sup>64</sup>.

Based on their studies, Sra et al (2010) investigated persistence kinetics in batch, column and push-pull field and demonstrated that oxidant decomposition rates increased from batch to column and field systems by 8 to 50 times, respectively <sup>67</sup>.

Kinetic data for the seven aquifer materials in the case of batch experiments using 20 g/L PDS concentration, showed that the unactivated PDS was stable in a remarkable range of concentrations. At 25 °C,  $k_{obs}$  showed that the PDS half-life was approximately around 600 days, but in presence of aquifer solids and different TOC contents, half-life was variable <sup>54</sup>.

Considering the case of site 1 and 3 in Table 1, where there was approximately a duplication in TOC content, half-life decrease was of 15.5 days, showing a higher stability in the case of lower TOC content. The same observation may be performed comparing site 3 and 5, in which once again it was visible a rise in half-life of 41.4 days due to the increase in TOC content. The results showed by Sra et al. (2010) showed how stability increase in presence of TOC due to their strong dependence.

*Table 1 - Total Organic Carbon content and half-life for 20 g/L PDS concentration in Sra et al. (2010) studies*

<b>Batch 20 g/L</b>		
<b>Site</b>	<b>TOC [mg/g]</b>	<b>Half-life [d]</b>
<b>1</b>	0.24	521
<b>2</b>	0.28	521
<b>3</b>	0.46	505.5
<b>4</b>	1.84	243.9
<b>5</b>	0.88	546.9
<b>6</b>	0.77	457.3
<b>7</b>	0.32	637.2

pH is another factor related to the production of  $H^+$ . The study demonstrated that during PDS degradation a decreasing from the initial pH is evident due to the generation of  $H^+$ . For this reason, a higher PDS degradation is related to a lower pH value. The decrease will be evident in systems with high concentrations of PDS, but in presence of aquifer materials the decrease in pH is not observed due to the buffering capacity of soils, that are able to resist to the changes in pH <sup>67</sup>. The buffering capacity of soils has a correlation with soil cation exchange capacity (CEC). The higher the CEC and buffering capacity, the smaller is the change in pH during PDS decomposition <sup>37</sup>.

#### **2.4.4 Persistence of activated peroxydisulfate in the presence of aquifer solids**

As discussed in paragraph 2.4.1, PDS activation is generally recommended to increase its oxidation potential and its reactivity with organic compounds <sup>67</sup>. Though the use of activators leads to an increase in system reactivity, the system persistence is influenced by the interaction of PDS with activators, reactive species each other and with aquifer materials <sup>54</sup>. Activations of PDS by  $H_2O_2$  or chelated- $Fe^{2+}$  lead to an increase in oxidation rates in target contaminants, but their applications influence the stability of the system and persistence conditions are not maintained. Therefore, stability is reduced compared to unactivated PDS. Once activating agents decreased, PDS degradation follows the unactivated PDS kinetics <sup>67</sup>.

The activation with  $H_2O_2$  is limited due to its rapid decomposition in the aquifer media. In presence of solids with high Fe content, the transport of the contaminant is limited. Higher is Fe content, higher will be the peroxide loss. Thus, there will be a slow degradation of PDS with a velocity similarly to the unactivated PDS. In the case of low Fe content, PDS stability will be lower due to the slow degradation of peroxide <sup>67</sup>.

Activation by  $Fe^{2+}$  accelerates the reactivity with target contaminants <sup>67</sup>. Due to the rapid oxidation of  $Fe^{2+}$  to  $Fe^{3+}$ , PDS degradation for low PDS concentrations is rapid. After the initial loss, the remaining part of PDS follows the first-order degradation kinetics and  $k_{obs}$  results four times higher than in the unactivated PDS. In laboratory, Sra et al (2010) have observed that in absence of solids the persistence of PDS is lower compared to the presence of aquifer solids <sup>54</sup>. In order to understand the loss of PDS and  $Fe^{2+}$ , it is necessary to consider the reaction rate coefficients  $k_1$  and  $k_2$ . The coefficient related to the formation of the sulfate radical ( $SO_4^{\bullet-}$ ) is  $k_1$  and  $k_2$  is related to the oxidation of  $Fe^{2+}$  in  $Fe^{3+}$ . A high  $k_1$  value implies low PDS stability, while a high  $k_2$  value implies loss of  $Fe^{2+}$  or activator strength <sup>67</sup>. To investigate about the persistence of activated PDS, CA is used. In their studies Sra et al (2010)

have demonstrated that the use of CA was not effective for the interaction between PDS and  $\text{Fe}^{2+}$ . The oxidation of  $\text{Fe}^{2+}$  led to a rapid reduction of the initial PDS concentration <sup>54</sup>.

In the  $\text{Fe}^{2+}/\text{S}_2\text{O}_8^{2-}$ /silt system, the activation has a high contribution for the SOM destruction, but high concentrations of  $\text{Fe}^{2+}$  can lead to the production of  $\text{SO}_4^{\cdot-}$  radicals that do not destroy SOM or organic compounds, but they decompose the additional amount of PDS increasing the SOD amount. In activated PDS systems the SOD concentration is higher than in unactivated PDS, because in unactivated system is not present the direct consumption of  $\text{Fe}^{2+}$  as in  $\text{Fe}^{2+}/\text{S}_2\text{O}_8^{2-}$  system <sup>64</sup>.

For the alkaline activation Sra et al (2010) have considered the use of hydroxide ( $\text{OH}^-$ ) in order to have a  $\text{pH} > 10$  <sup>67</sup>. However, the excess of  $\text{OH}^-$  can be positive for the degradation of organic compounds, but in the same time the total efficiency of the system can be compromised by it and can also limit the PDS stability. In order to maintain high pH values, it is necessary to control the acid production from PDS decomposition and the buffering capacity of aquifer sediments <sup>54</sup>.

Observing  $k_{obs}$  in activated PDS, it tends to be four times higher than for the unactivated PDS, but a loss in ionic strength is not present in the case of activated PDS. Similarly, to the unactivated case, PDS degradation is accelerated by ionic strength and the interactions with TOC and Fe. The latter is fundamental to establish the persistence of PDS <sup>54</sup>. Compared to the others activator, the alkaline activation has a lower impact on PDS persistence and stability <sup>67</sup>.

#### **2.4.5 Fundamentals using PDS – A resume**

PDS due to its solubility and high oxidation potential is one of the most widely oxidants used in ISCO technology. It can be activated in order to produce free radicals able to increase range applicability and degradation rate. The use of  $\text{H}_2\text{O}_2$ , chelated-ferrous and high pH has been proposed to be effective in PDS activation <sup>67</sup>. Compared with permanganate and  $\text{H}_2\text{O}_2$ , that are easily degraded in contact with soil and groundwater, PDS shows a higher stability in subsurface with a half-life of 100 to 500 days, factor that permits to degrade contaminants for a longer duration. On the other hand, it shows less affinity with NOM than permanganate and  $\text{H}_2\text{O}_2$  and therefore less SOD is required <sup>25</sup>. Since SOD depends on NOM and inorganic compounds content, it is necessary to evaluate soil properties in order to understand if PDS use is adequate and suitable in term of costs <sup>65</sup>.

Considering pH range effectiveness and alkalinity, it is important to point out that PDS can be applied in a wide pH range, but it is necessary to take into account the drop in pH values due to the sulfate production, the major inorganic byproduct of PDS reactions. A drop in pH will lead to a smaller ISCO effectiveness<sup>25</sup>. The latter can be affected also by a high scavenger's concentration that may have consequences on target organic contaminants oxidation. In particular, carbonate and bicarbonate that may slow down or totally inhibit contaminant degradation<sup>27</sup>.

Even some mechanisms are well understood, mainly in PDS activation, there are some aspects that still are not available, particularly regarding chemical processes able to degrade specific contaminants, especially those more resistant to oxidation (such as chloroethanes)<sup>27</sup>. A lack in factors that control the rate of PDS decomposition by aquifer materials exists. In addition the influence of TOC, Fe and Mn content is known to affect PDS decomposition<sup>57</sup>. Large uncertainty about PDS is also related to how subsurface interactions impact PDS stability, persistence and effectiveness<sup>27</sup>.

### 3 Materials and methods

In this section a description of the materials and methods used in the experiments is provided. The focus is placed on the aquifer materials used to prepare batch and column experiments and the procedure to achieve the objectives.

#### 3.1 Chemicals

Chemicals used include potassium iodide (KI, 99.5%, Penta, Czech Republic), sodium bicarbonate ( $\text{NaHCO}_3$ , 99.0%, Penta, Czech Republic) and sodium persulfate ( $\text{Na}_2\text{S}_2\text{O}_8$ , 99.0%, Penta, Czech Republic). Distilled water was used in all the experiments.

#### 3.2 Aquifer materials

Two well-characterized, uncontaminated aquifer materials collected from across Czech Republic (Nová Hůrka 49.1457111N, 13.3308447E, Prague – Holešovice 50.1066781N, 14.4178844E) (Figure 12, Figure 13) and one sea sand (Penta, Czech Republic) (Figure 14) were used in the experiments.



*Figure 12 - Soil 1*



*Figure 13 - Soil 2*



*Figure 14 - Sea sand*

### **3.3 Soils characteristics**

The soils used for the experiments, were properly dried exposing them to the air until a complete humidity stabilization. Once dried, the soil samples were analyzed to evaluate physical properties. Total Carbon (TC) and X-Ray Fluorescence (XRF) analysis were performed.

#### **3.3.1 Determination of Different Forms of Carbon**

TOC content is one of the indicators for ISCO applications designing. Measuring TOC directly is a non-trivial analysis. Regularly total carbon (TC) is measured, and then non-organic carbon sources are subtracted. Besides organic carbon, inorganic carbon also exists in soils and sediments, commonly in the form of carbonates. The corresponding bulk parameter, total

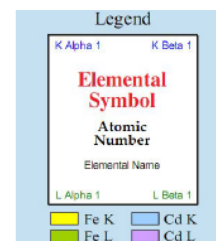
inorganic carbon (TIC), includes not only these minerals but also other carbonate derivatives, such as bicarbonate and carbonic acid. Furthermore, residual oxidizable carbon (ROC), hypothesized to be graphitic C is part of TC.

The different soils were grinded in a mortar to obtain fine powder. Determination of TOC in the soil samples was performed by determination of different forms of carbon via temperature programming using RC 612 (LECO, USA). The samples were introduced into the different temperature zones in the combustion furnace. Each zone corresponds to a different temperature which results in values for TOC400 at 400 °C, ROC at 600 °C and TIC900 at 900 °C.

### **3.3.2 Elemental composition**

The aquifer materials used in the experiments showed different properties and variation in composition. In order to determine the chemical properties, X-ray Fluorescence Spectrometry (XRF) was used.

XRF is an analysis technique based on the principle that individual atoms, when excited by an external energy source, emit X-ray photons of a characteristic energy or wavelength. By counting the number of photons of each energy emitted from a sample, the elements present can be identified and quantified <sup>69</sup>. Through this analysis it is possible to detect only certain elements of periodic table. Moreover, each element has a characteristic energy range of K and L shells, as shown in George Dowell periodic table (Figure 15).



3.31	3.59	3.69	4.01	4.09	4.45	4.51	4.93	4.95	5.43	5.41	5.95	5.90	6.49	6.40	7.06
<b>K</b>	<b>Ca</b>	<b>Sc</b>	<b>Ti</b>	<b>V</b>	<b>Cr</b>	<b>Mn</b>	<b>Fe</b>								
19	20	21	22	23	24	25	26								
Potassium	Calcium	Scandium	Titanium	Vanadium	Chromium	Manganese	Iron								
	0.34	0.34	0.39	0.40	0.45	0.46	0.51	0.52	0.57	0.58	0.64	0.65	0.70	0.72	
13.39	14.96	14.16	15.83	14.96	16.74	15.77	17.67	16.61	18.62	17.48	19.61	18.41	20.59	19.28	21.66
<b>Rb</b>	<b>Sr</b>	<b>Y</b>	<b>Zr</b>	<b>Nb</b>	<b>Mo</b>	<b>Tc</b>	<b>Ru</b>								
37	38	39	40	41	42	43	44								
Rubidium	Strontium	Yttrium	Zirconium	Niobium	Molybdenum	Technetium	Ruthenium								
1.69	1.75	1.81	1.87	1.92	2.00	2.04	2.12	2.17	2.25	2.29	2.40	2.42	2.54	2.56	2.68
30.97	34.96	32.19	36.38	Lanthanide Series		55.76	63.21	57.52	65.21	59.31	67.20	61.13	69.30	62.99	71.40
<b>Cs</b>	<b>Ba</b>			<b>Hf</b>	<b>Ta</b>	<b>W</b>	<b>Re</b>	<b>Os</b>							
55	56			72	73	74	75	76							
Cesium	Barium			Hafnium	Tantalum	Tungsten	Rhenium	Osmium							
4.29	4.62	4.47	4.83	7.90	9.02	8.15	9.34	8.40	9.67	8.65	10.01	8.91	10.35		

Figure 15 - George Dowell periodic table showing specific energy range for some elements

For example, the characteristic energy for Fe is: 6.40 keV for  $K_{\alpha}$  and 7.06 keV for  $k_{\beta}$ <sup>70</sup>.

The elemental composition of the materials was performed using ElvaX Mobile (Elvatech), a portable analyzer for testing a wide variety of materials. For each material, the XRF spectrum was measured first with no filter for lighter elements and then with aluminum filter with a thickness of 800 micrometers, for heavy metals and other heavier elements. Once the measure was performed, peak-up corrections were conducted on the spectra. To clean it, some characteristic elements of the instrument were deleted (Te, Ru, Rh, Cd, Ag). The elemental composition concentrations were evaluated by Uniquant 4 software that has provided the data in ppm.

### 3.4 Spectrophotometric determination of sodium persulfate concentration

In order to determine the sodium persulfate ( $\text{Na}_2\text{S}_2\text{O}_8$ ) concentration the spectrophotometry method was used. This method is used to estimate the concentration of an analyte in solution and it is based on the principle that materials absorb light of a certain wavelength as it passes through the solution. In order to measure the absorbance of a solution as light of specified wavelength that passed through it, spectrophotometer is used (Figure 16).

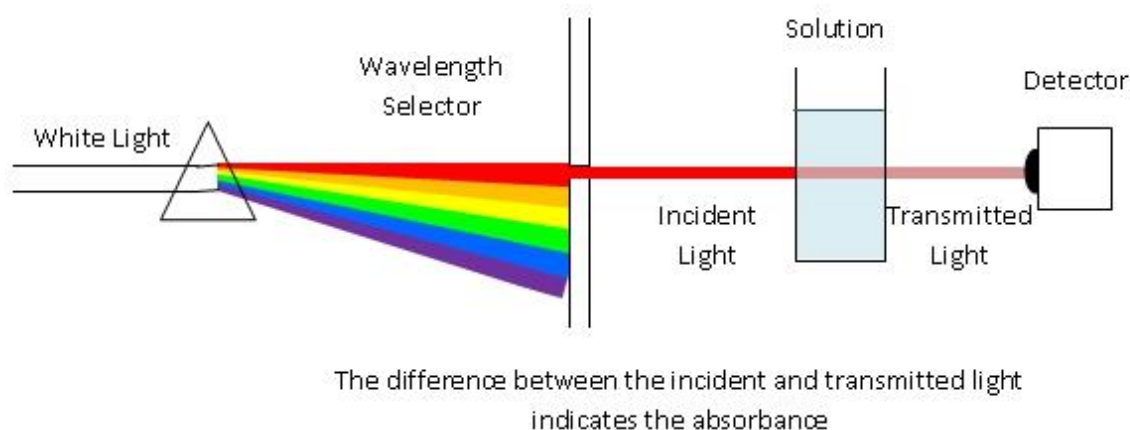


Figure 16 - Spectrophotometer principle

The principle is related to the Beer-Lambert law <sup>71</sup>:

$$A = l \cdot C \cdot \varepsilon$$

where,

- A is the absorbance;
- l is the optical path length (cm);
- C is the molar concentration (M);
- $\varepsilon$  is the molar absorption coefficient of the substance ( $M^{-1}cm^{-1}$ ).

Measuring the absorbance of the solution with a certain amount of analyte, it is possible to estimate its concentration <sup>71</sup>.

### 3.4.1 Calibration curve

The calibration curve was used to understand the instrumental response to PDS, and to determine the concentration of PDS in the samples. The calibration consists in a set of operations that relate the output of the measured system (absorbance) and the values of the calibration standards (the amount of the analyte present). The calibration requires the preparation of at least five standard solutions containing a known amount of the analyte of interest, measuring the response and establishing the relationship between the instrument response and analyte concentration <sup>72</sup>.

In this way it was possible to evaluate the amount of analyte present in the estimated samples. In the case of  $Na_2S_2O_8$ , the determination of concentration depends on the intensity of yellow

color measured in 400 nm from a reaction between  $\text{Na}_2\text{S}_2\text{O}_8$  and iodide anion in accordance with Eq.22:



### 3.4.1.1 Apparatus

The concentration of PDS was measured using Jasco V-530 UV-VIS Spectrophotometer (Jasco, Japan) with quartz glass cuvette with optical path 1 cm.

### 3.4.1.2 Procedure

Firstly, the agent with potassium iodide (KI) and sodium bicarbonate ( $\text{NaHCO}_3$ ) was prepared. The agent preparation was conducted measuring 25 g of KI and 6.25 g of  $\text{NaHCO}_3$  using laboratory scale. Once measured the amount of chemicals, they were transferred into 1 L volumetric flask and filled with distilled water until the mark. The agent was hand shaken and stored in a cool place.

Standard solutions were prepared as follows. The amount of  $\text{Na}_2\text{S}_2\text{O}_8$  (0.1 g) was measured using the analytical balance. Then it was transferred into 250 mL volumetric flask, with a concentration of 400 mg/L. Distilled water was used in order to fill the flask until the top line. Using a pipette, 25 mL of stock solution was collected and added into 100 mL volumetric with distilled water.

Calibration standards solutions have been prepared with six different concentrations (Table 2), including blank that contains none of the analyte (0 mg/L concentration) using the solutions prepared in the previous step. Different amounts of solutions were collected using the pipette and transferred into 50 mL volumetric flask, filled also with distilled water up the mark.

*Table 2 - Preparation of calibration solutions*

Calibration sol	Flask vol [mL]	Used sol	Pipetted vol [mL]	$\text{Na}_2\text{S}_2\text{O}_8$ conc. [mg/L]
blank	50	-	-	-
1	50	WS	2.5	5
2	50	WS	5	10
3	50	StS	2.5	20
4	50	StS	3.75	30
5	50	StS	5	40

Once prepared the calibration solutions (Figure 17), the absorbance of each sample was measured using the spectrophotometer and conducted at 400 nm (i.e., in the visible light wavelength range).



Figure 17 - Calibration solutions

After the instrument zero, the absorbance measurements were conducted. The back cuvette was filled with distilled water and the front with the different standard solutions.

To obtain calibration curve the measured absorbance was plotted against the known concentrations of standard solutions. To calculate the concentration of PDS in different samples regression line equation was used.

### 3.5 Batch experiments

To observe PDS degradation rates, batch reactor tests were prepared at low (1 g/L) and high (20 g/L) PDS concentrations. For each sample (1, 2, 3) the stock solutions with PDS in both the concentrations were prepared. The PDS amount (Table 3) was measured using an analytical balance. Once prepared the PDS, 500 mL of volumetric flasks with distilled water were used for the solutions.

Table 3 - Stock solutions for batch experiments for each sample (1, 2, 3) at 1 g/L and 20 g/L PDS concentration

Samples	PDS [g/L]
s-1-1	3.42
s-1-20	68.52
s-2-1	5.51
s-2-20	110.12
s-3-1	6.63
s-3-20	132.73

Once prepared the stock solutions, soil reactors and control reactors were prepared. Each soil reactor (300 mL) was filled with 100 g of aquifer solids and 100 mL of distilled water, except for soil 2, in which the amount of distilled water was 150 mL. The reactors were mixed mechanically for 24 hours (Figure 18, Figure 19). For each soil, three replicates were conducted.



*Figure 18 - Batch reactors*



*Figure 19 - Mixed batch reactors*

In the case of control reactors, they were filled with 50 mL of PDS and different amounts of distilled water, based on the sample. In this case, only one replicate was conducted.

Concerning PDS concentration, in the case of soil reactors it was measured after 5 and 10 days.

In the case of control reactors, it was measured at zero time, after 5 and 10 days.

The experiment design for all soils and control reactors, is showed below (Table 4):

Table 4 - Experiment design

	soil (g)	DW (mL)	PDS-1 (mL)	PDS-20 (mL)	number of replicates
Sample 1-1	100	100	50	x	I.-III.
Sample 1-20	100	100	x	50	I.-III.
Sample1-1c	x	121	50	x	I.
Sample1-20c	x	121	x	50	I.
Sample 2-1	100	100	50	x	I.-III.
Sample 2-20	100	100	x	50	I.-III.
Sample2-1c	x	225	50	x	I.
Sample2-20c	x	225	x	50	I.
Sample 3-1	100	100	50	x	I.-III.
Sample 3-20	100	100	x	50	I.-III.
Sample3-1c	x	116	50	x	I.
Sample3-20c	x	116	x	50	I.

### 3.5.1 PDS concentration

#### 3.5.1.1 Dilutions

To evaluate PDS concentration using spectrophotometry, it was necessary to dilute first the samples. Serial dilutions were used in a succession of step dilutions, where the diluted material of the previous step was used to make the subsequent dilution.

##### 3.5.1.1.1 Controls

For the controls, in the case of high concentration (20 g/L), the dilution was performed in two steps. In the first step 5 mL of the sample were collected using a pipette and transferred into 250 mL volumetric flask. Distilled water was used until the mark. The second step provided the collection of 10 mL with the pipette and the transfer into 100 mL volumetric flask, using distilled water. The solution for the spectrophotometry was prepared putting in 50 mL volumetric flask the sample (5 mL), the agent (40 mL) and distilled water (5 mL).

Evaluating the dilution factor (DF) as the ratio between the final volume (volumetric flask) and the initial volume (sample), it was possible to calculate DF for each step (Table 5).

*Table 5 -Dilution factor (20 g/L)*

<b>Step</b>	<b>Initial volume [mL]</b>	<b>Final volume [mL]</b>	<b>DF</b>
<b>1</b>	5	250	50
<b>2</b>	10	100	10
<b>Final solution</b>	5	50	10

Multiplying each DF, the total DF for 20 g/L was 5000.

For low concentration (1 g/L) the dilution took place in one step. With a pipette, 4 mL of the sample were transferred into 100 mL volumetric flask and distilled water was used. The final solution for the measures was prepared as seen above. The DF was also calculated (Table 6).

*Table 6 - Dilution factor (1 g/L)*

<b>Step</b>	<b>Initial volume [mL]</b>	<b>Final volume [mL]</b>	<b>DF</b>
<b>1</b>	4	100	25
<b>Final solution</b>	5	50	10

The total DF in this case was 250.

Once prepared the solutions to analyze with spectrophotometer, they were hand shaken and allowed to equilibrate for 15 min.

### **3.5.1.1.2 Soils reactors**

The dilution for the three samples containing the three different kind of soils, followed the same procedure as for the controls. For both high and low PDS concentration, the dilution step was only one.

For 20 g/L, using a pipette 0.5 mL of aqueous sample were transferred into 200 mL volumetric flask and distilled water was used. The solution was prepared as seen in 3.5.1.1.1. The total DF was 2000 (Table 7).

*Table 7 - Dilution factor (20 g/L)*

<b>Step</b>	<b>Initial volume [mL]</b>	<b>Final volume [mL]</b>	<b>DF</b>
<b>1</b>	0.5	200	200
<b>Final solution</b>	5	50	10

In the case of 1 g/L, with the pipette 0.5 mL were collected and moved into 50 mL volumetric flask. Distilled water was used until the mark. The final solution was prepared. The total DF was 1000 (Table 8).

Table 8 - Dilution factor (1 g/L)

Step	Initial volume [mL]	Final volume [mL]	DF
1	0.5	50	100
Final solution	5	50	10

In order to perform the dilutions for the soil 1 was necessary to use a filter (0.45  $\mu\text{m}$ ) to eliminate the impurities into the soil (Figure 20). Firstly, with a syringe, an amount of sample (1 mL) was collected from the batch and filtered.



Figure 20 - Filter (0.45  $\mu\text{m}$ )

Soil 3 (Figure 21), showed a large amount of organic substances and for this reason was complicated to collect easily amounts of aqueous samples.



Figure 21 - Batches soil 2

In order to allow the settling of the soil impurities was necessary to use a centrifuge. An amount of sample (1 mL) was collected and the centrifuge (Figure 22), with a velocity of 10000 rpm, was used for 5 min.

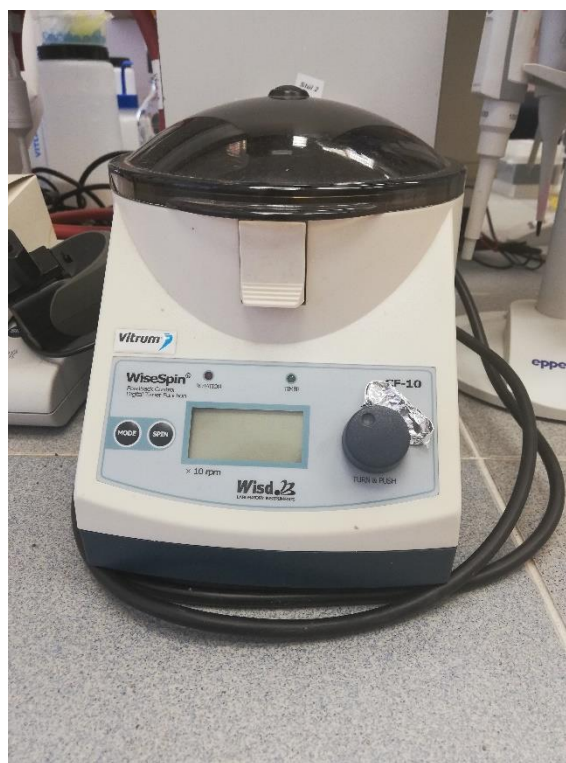


Figure 22 – Centrifuge

Once prepared the final solutions, the volumetric flask was hand shaken and 15 min were necessary to allow the equilibrium.

### 3.6 Column experiments

The columns used for the experiments were Plexiglas (4.8 cm inner diameter x 40 cm length). Sample 1 and 3 were used for columns experiments in order to evaluate the decomposition rates as close as possible to in situ conditions. The columns were prepared adding to the bottom some compacted gravel in order to achieve homogenous flow. Then the dry soil and distilled water were added carefully, in order to avoid the formation of empty spaces. Reached the top of the column, the last 3 cm were filled with the same compact material of the bottom.

Knowing the amount of distilled water added in the two columns, the calculation of the pore volume (PV) was possible. In the case of sample 1 the PV was 370 mL, for the sample 3 resulted 260 mL. Distilled water (1 L) was flushed through the columns (6 pore volumes) for 3 days using Tygon or Teflon tubing and peristaltic pump (Ismatec 123) (Figure 23).



*Figure 23 - Column experiment*

6 pore volumes of high PDS concentration solution were injected into the column in up-flow mode at a flow rate of  $\sim 5$  mL/min to establish a uniform initial PDS concentration throughout the column. Once that the graduated cylinder was filled, the samples were stored in order to evaluate, consequently, the absorbance. Achieved the breakthrough (effluent concentration 20 g/L), the injection was stopped, and the tubing at both ends of the columns was clamped. The samplings were used for the measure of PDS concentration and degradation rates.

Following this initial water saturation process, PDS with high concentration flushed into the columns (Figure 24).



Figure 24 - PDS flow into the columns

Breakthrough curves were plotted using Ogata-Banks's solution (Eq.23):

$$\frac{C}{C_0} = \left\{ \operatorname{erfc} \left( \frac{x - v_{eff}t}{2\sqrt{D_x t}} \right) + \exp \left( \frac{v_{eff}x}{D_x} \right) \operatorname{erfc} \left( \frac{x + v_{eff}t}{2\sqrt{D_x t}} \right) \right\} \quad (23)$$

Porosity measures were conducted in order to understand the physical properties of the two soils. Considering the volume of water into the pores total volume of the column, porosity was calculated as follow:

$$\varepsilon = \frac{V_w}{V_T}$$

### 3.7 Statistical analysis

Three replicates were done in both batch and column experiments. The average ( $\bar{C}$ ) and the standard deviation ( $\mu_C$ ) (Eq. 23) of the PDS concentration within the replicates were calculated to determine the normalized remaining concentration (NRC) of PDS through time (Eq. 24). The results for PDS degradation are shown using the NRC, which standard deviation was calculated using Eq.25.

$$\mu_C = \sqrt{\frac{\sum_{i=1}^n (C_i - \bar{C})^2}{n(n-1)}} \quad (23)$$

$$\text{NRC} = \frac{\bar{C}}{\bar{C}_0} \quad (24)$$

$$\mu_{\text{NRC}} = \frac{\bar{C}}{\bar{C}_0} \sqrt{\left(\frac{\mu_C}{\bar{C}}\right)^2 + \left(\frac{\mu_{C_0}}{\bar{C}_0}\right)^2} \quad (25)$$

## 4 Results and discussions

In the present section the data obtained from the laboratory experiments concerning the PDS decomposition are reported.

### 4.1 Properties and composition

In order to characterize the soils Total Carbon (TC) were measured and X-Ray Fluorescence (XRF) analysis was performed in order to evaluate the particle's elemental composition.

#### 4.1.1 Total Carbon

Total carbon (TC) content is an important information that is needed for the analysis of the carbon content in a sample. In detail, in this study was fundamental to analyze TC content in order to determine NOD, defined as the oxidant that is consumed by organic and inorganic components in soil matrix. For this purpose it is necessary to analyze TC content since it usually consumes PDS before contaminant oxidation proceeds <sup>73</sup>.

The measurement of TC is related to the total organic carbon (TOC) content and total inorganic carbon (TIC) content by:

$$TC = TOC + TIC$$

In order to determine the carbon content of the samples, one of the components of organic matter, TOC and TIC content for each soil were measured. In this way the measurement of TC was obtained. Analysis of TC, TOC and TIC for each soil is provided in Table 9.

For each sample the measure was conducted in triplicate considering three total weight of the three samples.

*Table 9 – Results of Total Carbon (TC), Total Organic Carbon (TOC), Residual Oxidizable Carbon (ROC), Total Inorganic Carbon (TIC) referred to the three analyzed samples (S1, S2, S3). Measure were conducted in triplicate (1, 2, 3) considering for the same sample three total weights.*

<b>Samples</b>	<b>Weight (mg)</b>	<b>% TC</b>	<b>% TOC</b>	<b>% ROC</b>	<b>% TIC</b>
<b>S1 1</b>	212.47	3.81	3.05	0.50	0.26
<b>S1 2</b>	199.48	3.79	3.00	0.53	0.26
<b>S1 3</b>	211.33	3.87	3.09	0.51	0.27
<b>S2 1</b>	201.87	13.0	11.39	1.51	0.11
<b>S2 2</b>	202.17	12.7	11.10	1.46	0.10
<b>S2 3</b>	194.51	12.9	11.31	1.45	0.10
<b>S3 1</b>	180.52	-	-	-	-
<b>S3 2</b>	158.72	-	-	-	-
<b>S3 3</b>	171.17	-	-	-	-

Analyzing the data obtained, the TOC in both sample 1 and 2, does not differ too much from TC, while the TIC content is only a small fraction of TC. As evident, also ROC measure is considered. As specified before, it is referred to the graphitic C that constitutes only a small fraction. Experiments on soil 2 showed a significant amount of TC (~ 12.9 %) that may involve in a higher dependence in PDS rate decomposition. In the case of sample 3, Table 9 shows an absence in obtained data due to the absence of TOC in the sand chosen.

#### **4.1.2 X-Ray Fluorescence analysis**

To characterize the samples from a chemical-mineralogical point of view, XRF analysis was conducted. In detail, XRF analysis was able to identify the concentrations of the elements present in soil samples. The results obtained from the analysis are represented in a graph, called spectra, showing on the x-axis the X-rays energy emitted from the examined material and on y-axis the intensity of the rays. Particularly, for each sample it was possible to obtain two spectra: the first one measured with no filter and the second with an aluminum filter, in order to have evidence on heavy metals. In this way was possible to detect the responsible elements related with PDS decomposition in time and mainly investigate about Fe and Mn concentrations.

Considering the concept defined in 3.3.2 according to which each element has a characteristic energy range and observing Figure 25 to Figure 30 and in particular, Fe X-ray energy on x-axis, it is evident that the values obtained by the analysis were respecting the values showed in the specific periodic table showed in Figure 15.

The elemental composition is reported in Table 10.

Analyzing the spectra, for each sample specific results were reached:

- Soil 1 spectra (Figure 25, Figure 26) showed a high content of Fe, Si, K, Ca and Ti, but with the aluminum filter application it was evident a significant Fe and Mn content, the two elements of major interest for this study;

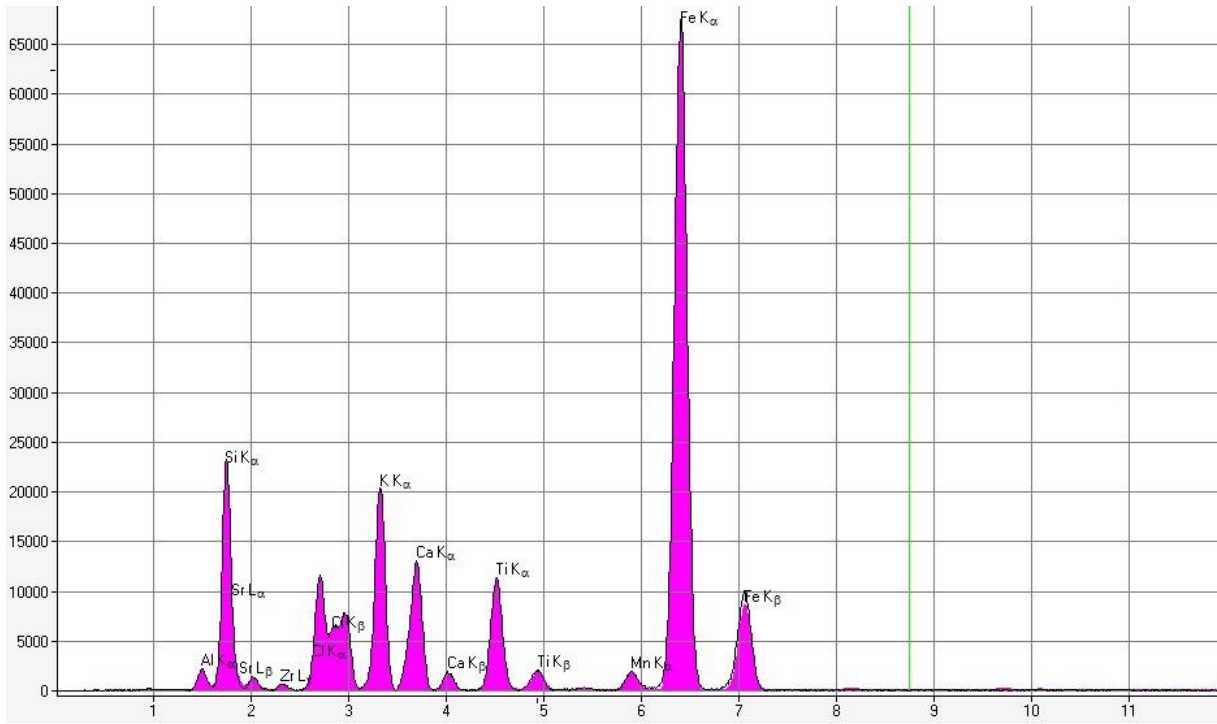


Figure 25 - Soil 1 spectra, no filter

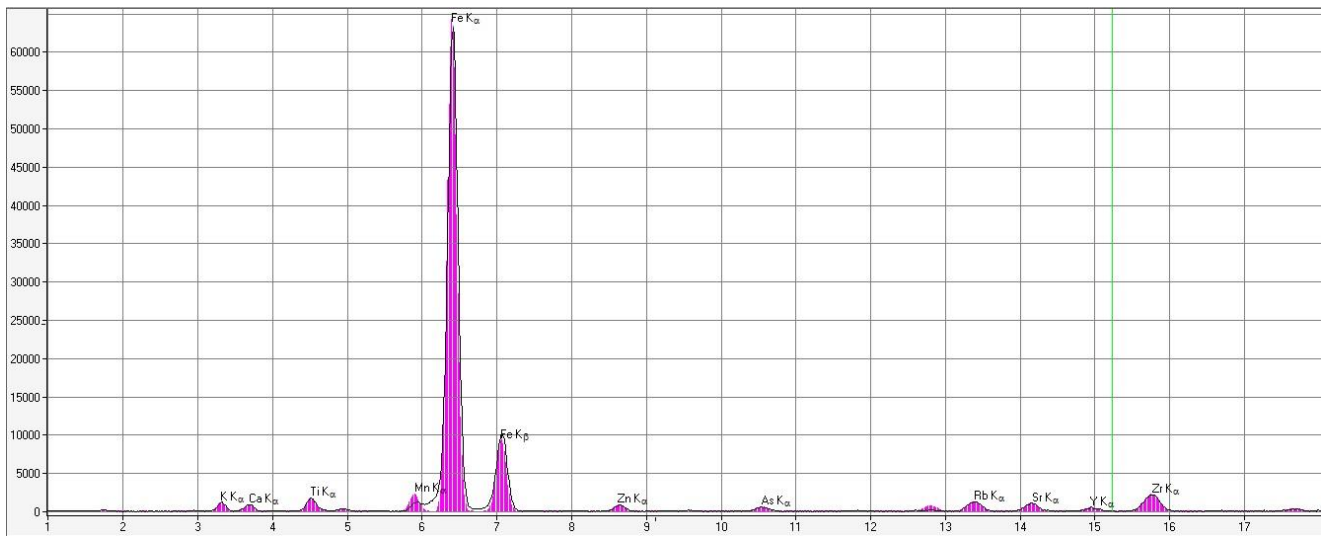


Figure 26 - Soil 1 spectra, with Al filter

- Soil 2 spectra (Figure 27, Figure 28) showed a similar situation. The elements present in higher content were Fe, Ca, Ti, K and Si, but by referring to the filtered spectra, it was considerable the high presence in Fe and Mn concentrations. There is no evident difference between soil 1 and 2 referring to elemental composition of the soil.

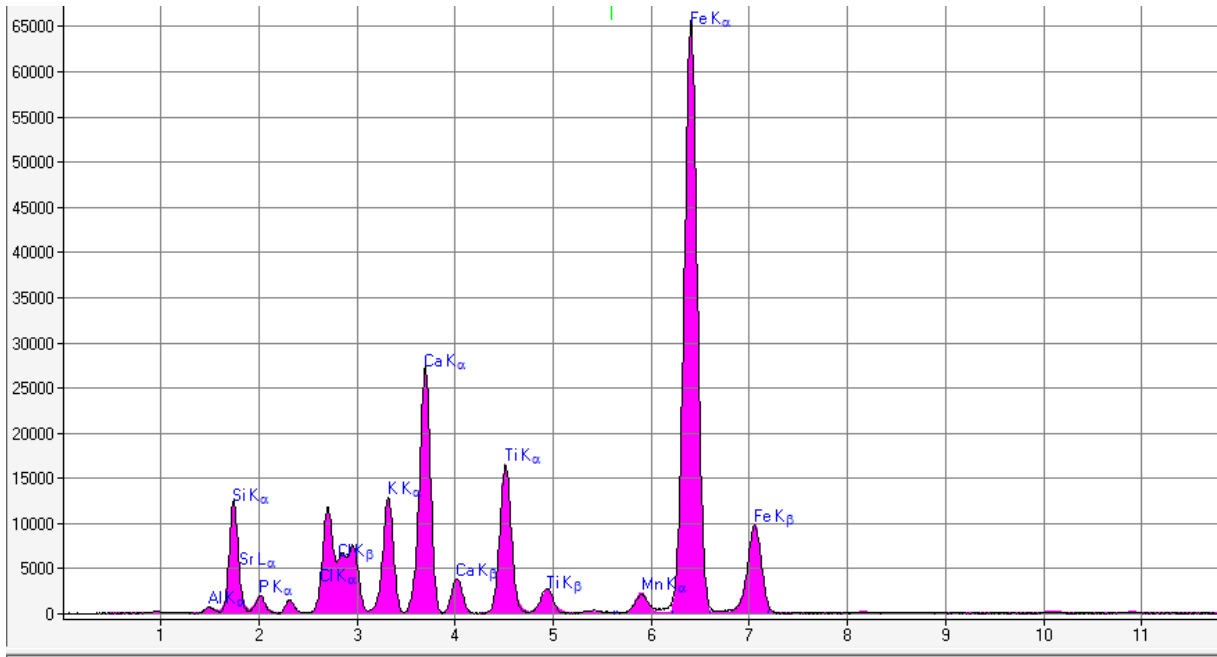


Figure 27 - Soil 2 spectra, no filter

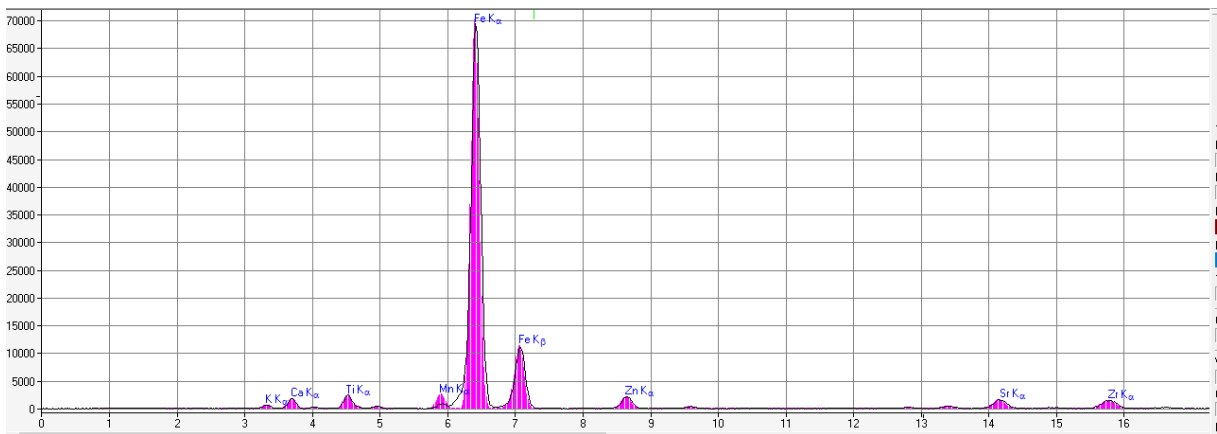


Figure 28 - Soil 2 spectra, with Al filter

- Soil 3 (Figure 29, Figure 30) confirmed to be a sand due to the high Si content in both spectra. It is noticeable also a Cl content in the spectra with no filter, as shown in the Figure 28.

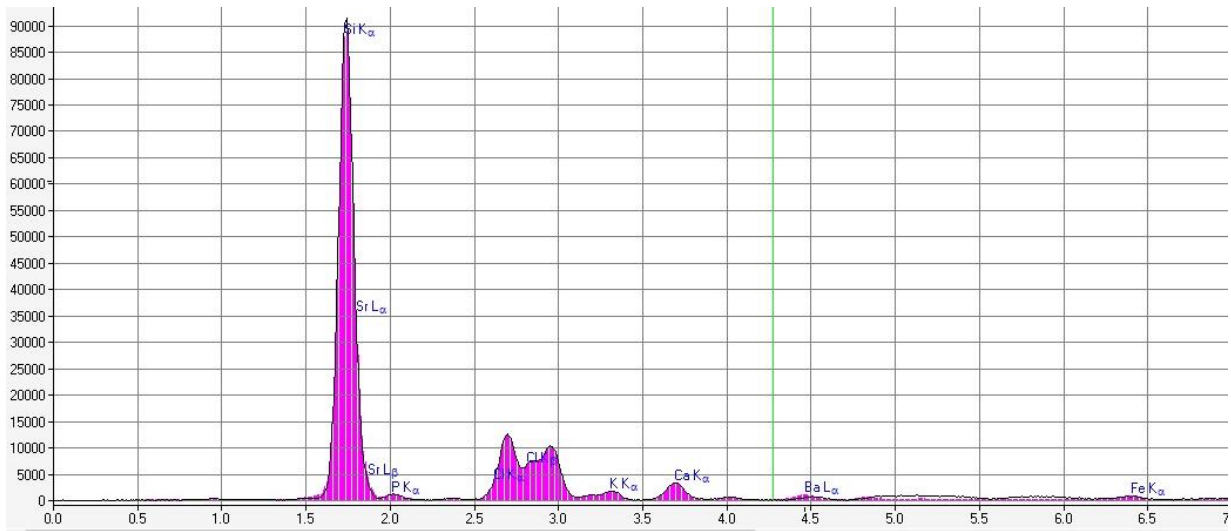


Figure 29 - Soil 3 spectra, no filter

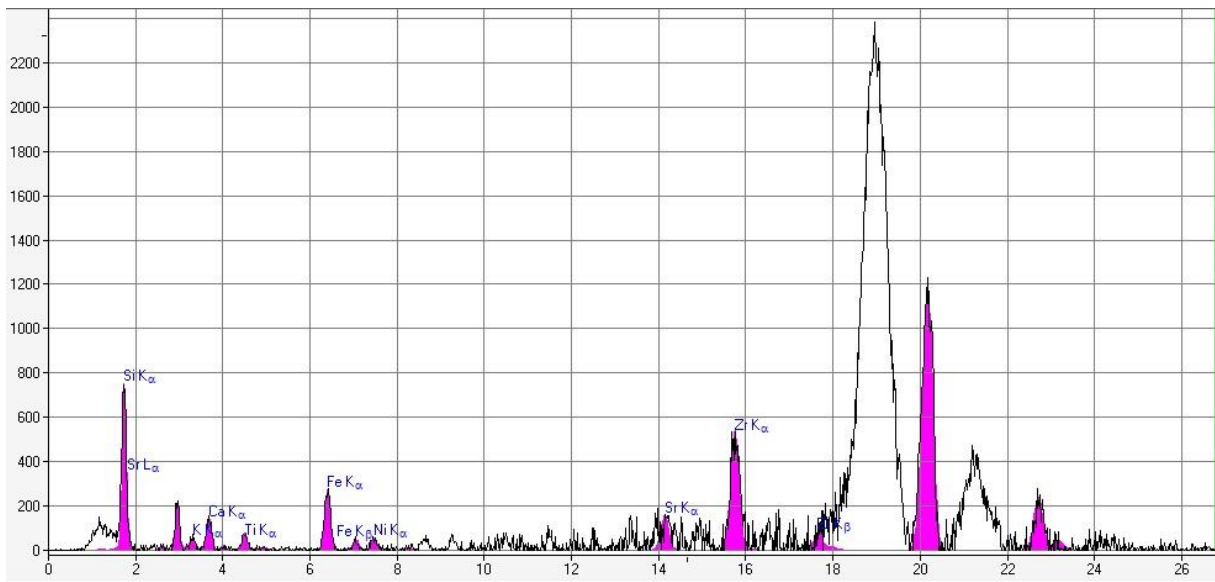


Figure 30 - Soil 3 spectra, with Al filter

Table 10 - Elemental composition obtained from XRF analysis in ppm

Element	Concentration (ppm)		
	S1	S2	S3
Si	196130 ± 873	136025 ± 957	773811 ± 1132
K	64376 ± 357	47705 ± 413	15950 ± 596
Cl	56333 ± 928	68010 ± 1183	177160 ± 2439
Fe	49096 ± 184	66581 ± 248	< 1
Al	27309 ± 845	9635 ± 919	-
Ca	22515 ± 190	59761 ± 301	14772 ± 326
Ti	7028 ± 202	11668 ± 284	< 1
Mn	2863 ± 49	3960 ± 64	-

For some elements present in the three different samples, the results have not been reported because their concentrations were not significant.

## 4.2 Determination of PDS concentration

### 4.2.1 Calibration curve

A calibration curve was used in order to understand the instrumental response to the analyte and predict the concentration of analyte in the samples. After the preparation of the standard solutions and the blank, the absorbance was measured. In order to plot the graph, the difference between the absorbance in the different samples and blank absorbance was conducted. Data for the graph plotting are shown in Table 11. The calibration curve is shown in Figure 31.

Table 11 - Calibration curve data

Standard solutions	Abs	C [mg/L]
blank	0.0013	0
1	0.1322	5
2	0.2839	10
3	0.5633	20
4	0.8453	30
5	1.1212	40

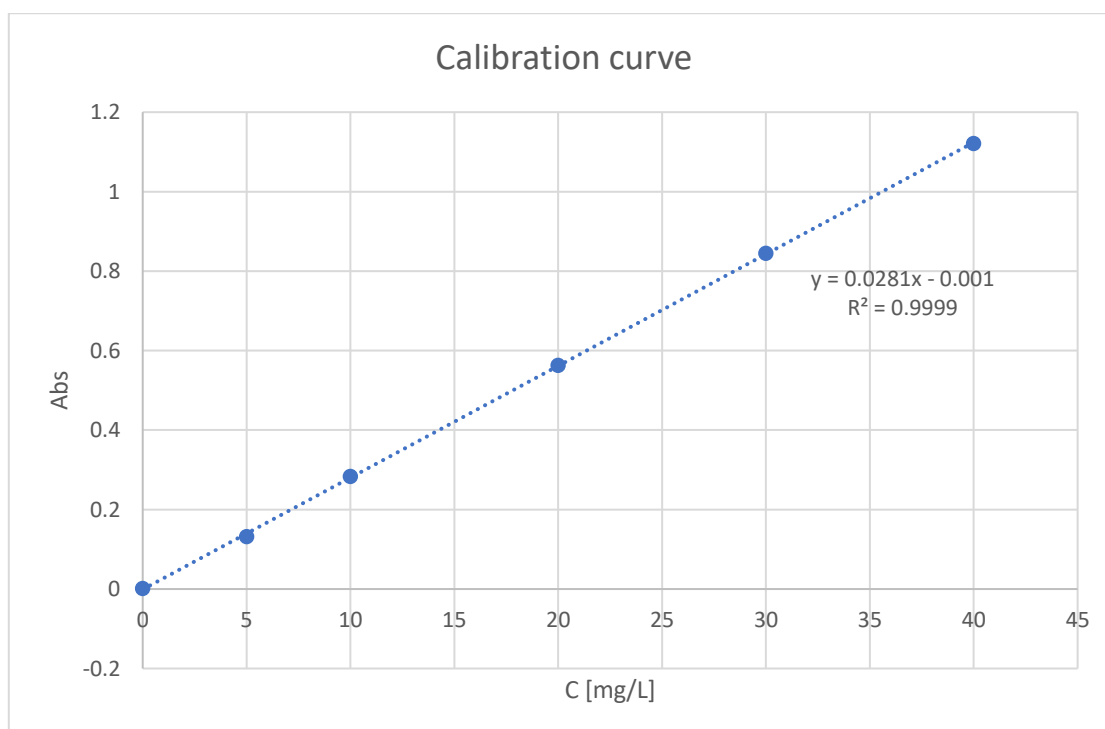


Figure 31 – Calibration curve

As expected, the more intensely colored solutions were characterized by a higher absorbance, related to the higher PDS concentration.

As evident the curve was a straight line with a linear equation, where 0.0281 is the slope of the line. Moreover, the  $R^2$  value (0.9999) showed that the data used to generate the calibration curve is very linear and that it is well described by Beer's law.

Using the linear equation shown in the figure, PDS concentrations in the analyzed samples were calculated, considering the maximum working range until 40 mg/L.

#### 4.2.2 Batch experiments

The PDS degradation through the three different samples was tested using batch experiments as described in chapter 3.5. The study was conducted at low and high PDS concentration (1 g/L and 20 g/L). All the samples were diluted before proceeding with the measurement of PDS concentration, in order to respect the working range obtained from the calibration curve. As an example, below the solutions after 5 days for samples 1, 2 and 3:

- sample 1



*Figure 32 - Sample 1 solutions after 5 days at 1 g/L PDS concentration*



*Figure 33 - Sample 1 solution after 5 days at 20 g/L PDS concentration*

- sample 2

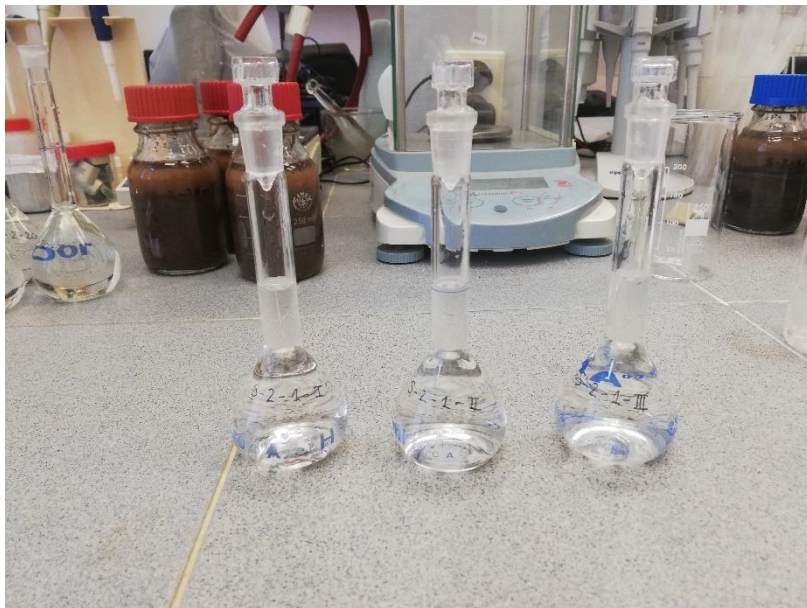


*Figure 34 - Sample 2 solution after 5 days at 1 g/L PDS concentration*

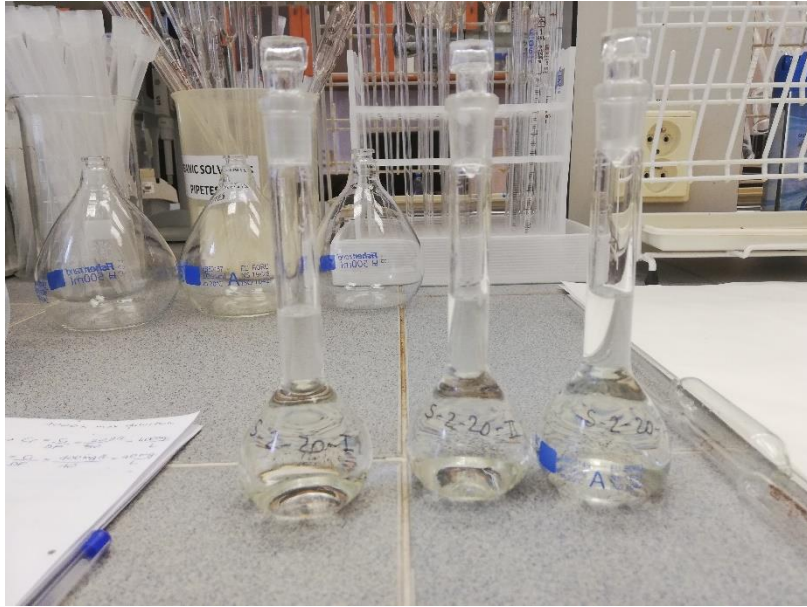


Figure 35 - Sample 2 solution after 5 days at 20 g/L PDS concentration

- sample 3



Figure 36 - Sample 3 solution after 5 days at 1 g/L PDS concentration



Figure 37 - Sample 3 solution after 5 days at 20 g/L PDS concentration

### 4.2.2.1 Control reactors

During the experimental period (~10 days), in order to analyze PDS degradation in time, the behavior of PDS was evaluated in control reactors, consisting of PDS at two concentrations in distilled water only. Data from the control reactors for both low and high concentration are shown in Table 12 and the respective graphs in Figure 38-Figure 39.

Table 12 - Control reactors data referred to the three samples (s1, s2, s3) respectively at 1 g/L and 20 g/L of PDS concentration (1c, 20c). Measures performed at zero time, after 5 and 10 days.

Time [days]	Controls [mg/L]					
	s1-1c	s2-1c	s3-1c	s1-20c	s2-20c	s3-20c
0	820.28	879.00	1666.37	12117.44	16316.73	27953.74
5	820.28	548.04	1449.29	15907.47	17597.86	29003.56
10	859.43	865.66	1603.20	23914.59	19555.16	25391.46

Figure 38 below indicates that for soil 1 and 3, at low concentration (1 g/L) PDS was stable for the entire period of 10 days, there is no evident reaction between PDS and the solution due to the absence of soils.

An exception is evident in the case of sample 2: there is not a stable behavior in time in PDS concentration, but a not clear rise in PDS concentration over time.

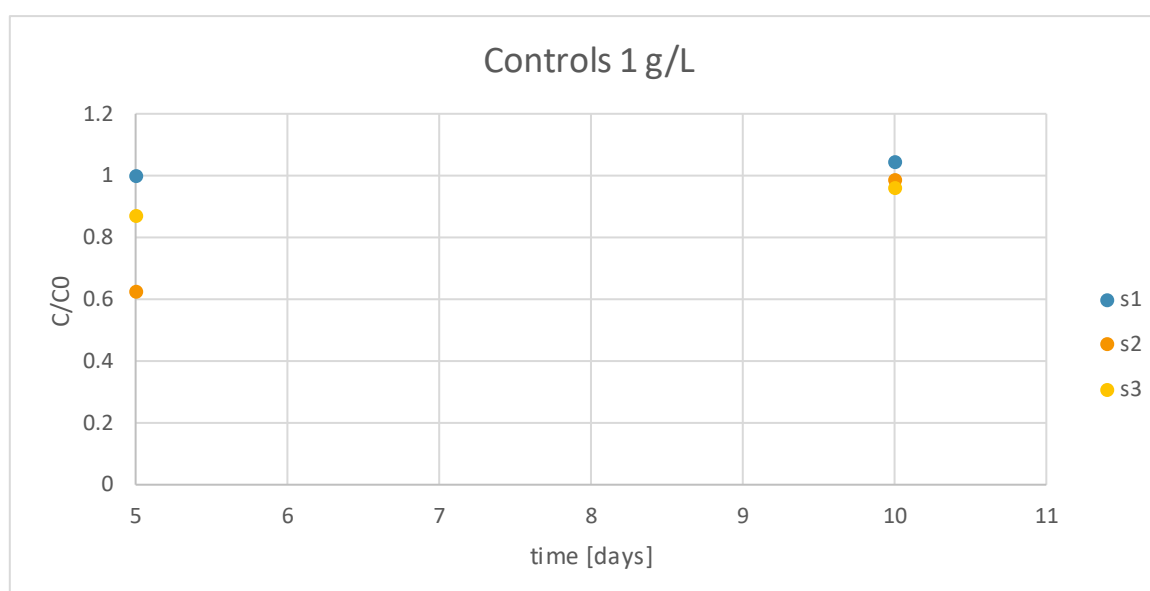


Figure 38 - Control reactors data referred to the three samples (s1, s2, s3) for the entire experiment duration (10 days). Data refers to 1 g/L PDS concentration.

Figure 39 shows that PDS at high concentration was stable until the end of the experiments for both sample 2 and 3, because of the absence of reactivity between the oxidant and the soil. In Figure 39 it is evident an unusual behavior in sample 1, showing an increase in PDS concentration between day 5 and 10. It was an anomalous trend since there may be no reaction between the samples and distilled water.

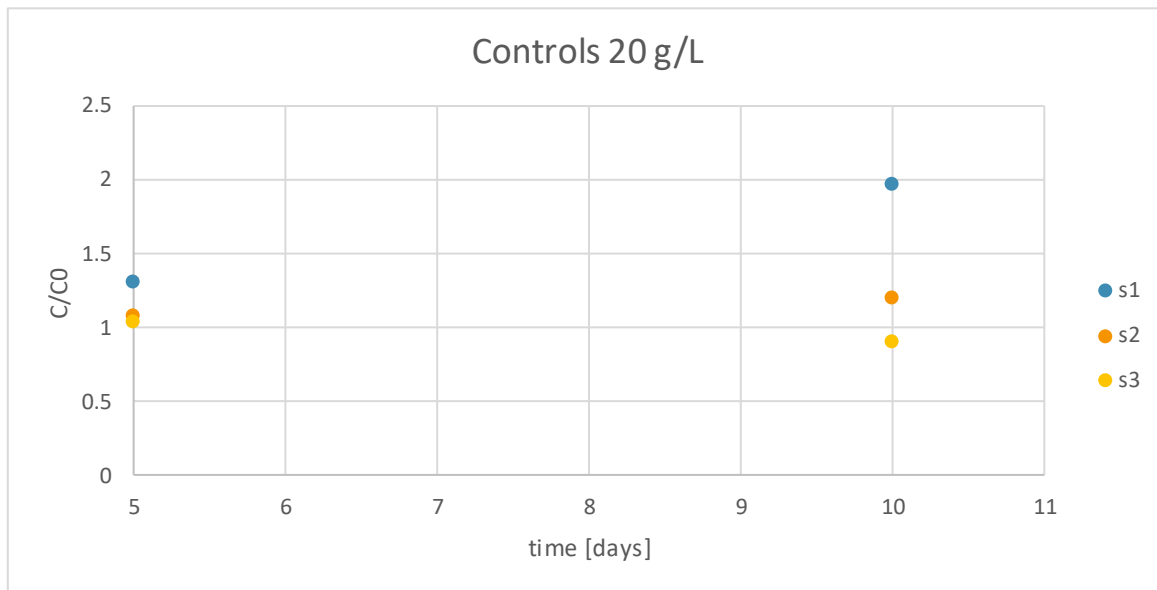


Figure 39 – Control reactors data referred to the three samples (s1, s2, s3) for the entire experiment duration (10 days). Data refers to 20 g/L PDS concentration.

#### 4.2.2.2 Sample reactors – Kinetic approach

##### 4.2.2.2.1 Low PDS concentration

For each sample, the measures were conducted after 5 and 10 days in triplicate for each PDS concentration (1 g/L and 20 g/L), collecting the samples three times from the corresponding batch so that was possible to obtain three PDS concentration values. The average of PDS concentration and the standard deviation were calculated.

Table 13, Table 14, Table 15 show the results obtained from batch experiments related to the lower PDS concentration (1 g/L) for each sample. For a better interpretation of the results, PDS concentration profiles were plotted in a graph (Figure 40) considering the ratio  $C/C_0$  versus time. For time zero each standard deviation resulted equal to zero because the measures of PDS concentrations were conducted immediately after 5 and 10 days.

Table 13 – Average of PDS concentration, Standard Deviation, C/C<sub>0</sub> and C/C<sub>0</sub> Standard Deviation for Sample 1 (1 g/L PDS concentration)

<b>Time [days]</b>	<b>Average PDS [mg/L]</b>	<b>Standard deviation</b>	<b>C/C<sub>0</sub></b>	<b>Standard deviation C/C<sub>0</sub></b>
<b>0</b>	820.2847	0	1	0
<b>5</b>	844.6026	77.5060	1.0296	0.1336
<b>10</b>	570.5813	174.4982	0.6956	0.2221

Table 14 - Average of PDS concentration, Standard Deviation, C/C<sub>0</sub> and C/C<sub>0</sub> Standard Deviation for Sample 2 (1 g/L PDS concentration)

<b>Time [days]</b>	<b>Average PDS [mg/L]</b>	<b>Standard deviation</b>	<b>C/C<sub>0</sub></b>	<b>Standard deviation C/C<sub>0</sub></b>
<b>0</b>	879.004	0	1	0
<b>5</b>	578.885	359.0663	0.6586	0.57770
<b>10</b>	295.374	126.5223	0.3360	0.25330

Table 15 - Average of PDS concentration, Standard Deviation, C/C<sub>0</sub> and C/C<sub>0</sub> Standard Deviation for Sample 2 (1 g/L PDS concentration)

<b>Time [days]</b>	<b>Average PDS [mg/L]</b>	<b>Standard deviation</b>	<b>C/C<sub>0</sub></b>	<b>Standard deviation C/C<sub>0</sub></b>
<b>0</b>	1666.370	0	1	0
<b>5</b>	2367.734	147.7761	1.4208	0.125
<b>10</b>	2069.988	180.6671	1.2422	0.133

Analyzing the data from a kinetic point of view, it was evident that after the first injection of PDS into the samples, there was a different behavior in the three soils in term of PDS concentration. In general, considering the values obtained plotting the natural logarithm of PDS concentration versus time, it was evident that the process is described by a first-order rate law. k values were obtained considering the line slope.

Figure 40 shows that data from sample 1, after the first five days, indicated that PDS at low concentration (1 g/L) was stable over time (SD ~ 9%). Until the end of the experimental period (10 days), the PDS reacted slowly, leading to little PDS decomposition and with an estimated first-order rate coefficient of  $7.8 \times 10^{-2} \text{ d}^{-1}$  and half-life of 8.84 d. The slow reaction between PDS and the soil was due to the low TOC content observed and to the sufficient content of Fe and Mn in its elemental composition, that are known as the major factors influencing PDS decomposition rates.

The faster PDS degradation in time was visible in Figure 40 for sample 2. During the entire experimental period, it was possible to notice a remarkable degradation velocity showing an exponential decay over time. The first-order coefficient was estimated equal to  $0.1346 \text{ d}^{-1}$ , corresponding to a half-time of 5.14 d. The results are consistent with the theory by which the PDS is consumed by the reaction with soil and particularly, with soil rich in TOC (as in this case) and in Fe and Mn content.

In the case of sample 3, Figure 40 shows a completely different situation. It was possible to notice an absence of reaction with PDS, likely due to the absence of organic content and a very low Fe content ( $< 1 \text{ ppm}$ ), two fundamental elements that determine persistence and stability of PDS. This is coherent with the literature, reporting that in sandy soils PDS shows a great persistence that permits to obtain major results in contaminants degradation and a higher remediation efficiency.

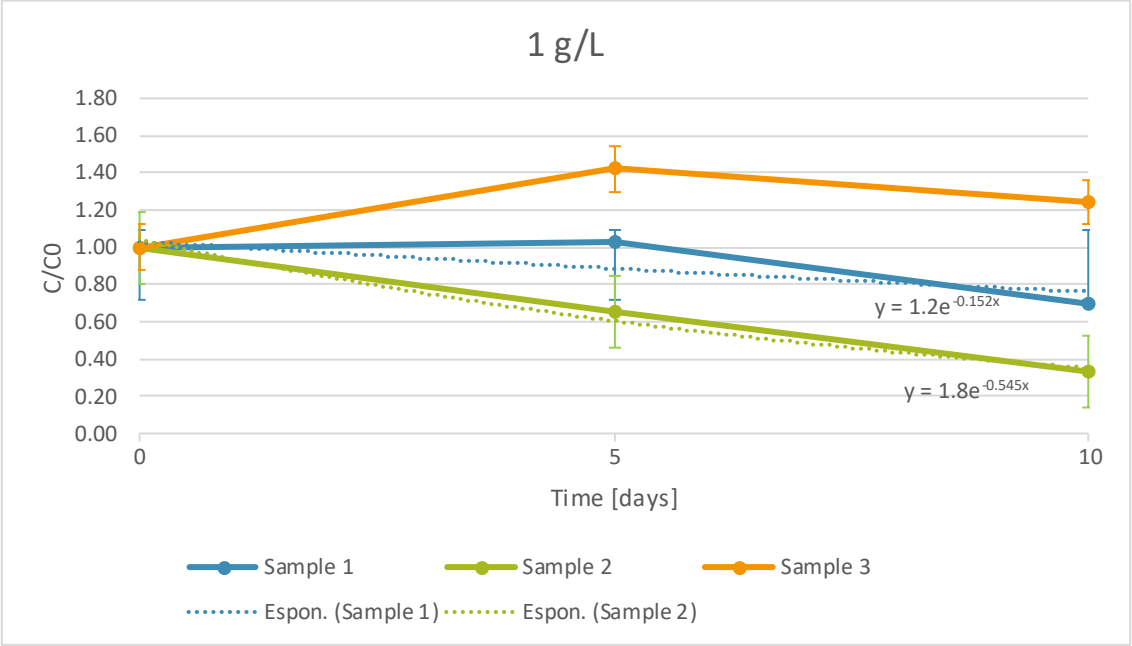


Figure 40 - PDS concentration profile for the three samples. PDS initial concentration 1 g/L

#### 4.2.2.2.2 High PDS concentration

Concerning the high PDS concentration (20 g/L), the results obtained from the laboratory experiments are shown in Table 16, Table 17, Table 18 for each sample:

Table 16 - Average of PDS concentration, Standard Deviation,  $C/C_0$  and  $C/C_0$  Standard Deviation for Sample 1 (20 g/L PDS concentration).

Time [days]	Average PDS [mg/L]	Standard deviation	$C/C_0$	Standard deviation $C/C_0$
0	12117.44	0	1	0
5	16465.01	494.77	1.3588	0.0577
10	9233.69	4046.29	0.7620	0.3347

Table 17 - Average of PDS concentration, Standard Deviation,  $C/C_0$  and  $C/C_0$  Standard Deviation for Sample 2 (20 g/L PDS concentration).

Time [days]	Average PDS [mg/L]	Standard deviation	$C/C_0$	Standard deviation $C/C_0$
0	16316.73	0	1	0
5	1762.75	523.73	0.1080	0.0454
10	1774.614	1774.61	0.1088	0.0897

Table 18 - Average of PDS concentration, Standard Deviation,  $C/C_0$  and  $C/C_0$  Standard Deviation for Sample 3 (20 g/L PDS concentration).

Time [days]	Average PDS [mg/L]	Standard deviation	$C/C_0$	Standard deviation $C/C_0$
0	27953.74	0	1	0
5	41976.28	1349.58	1.5016	0.0682
10	41530.25	2583.88	1.4856	0.1042

Plotting PDS concentration over time (Figure 41) its decomposition in time showed a different behavior for the three different samples.

In the first sample, after five days it is possible to approximate the PDS decomposition as stable, followed by a slight decomposition in time until ten days. The reaction rate in this case was  $0.1157 \text{ d}^{-1}$ .

Analyzing sample 2, a rapid decomposition in time was visible for the first five days, but in contrast to the other case, the graph shows that from the day five until the day ten, the PDS concentration remained stable over time. Evaluating the reaction rate coefficient, equal to 0.13

$\times 10^{-2} \text{ d}^{-1}$ , also in this case turned out an exponential decay. Considering an absence of reactivity with PDS, for sample 3, there was no evident degradation for the first five days, followed by stability of PDS over time.

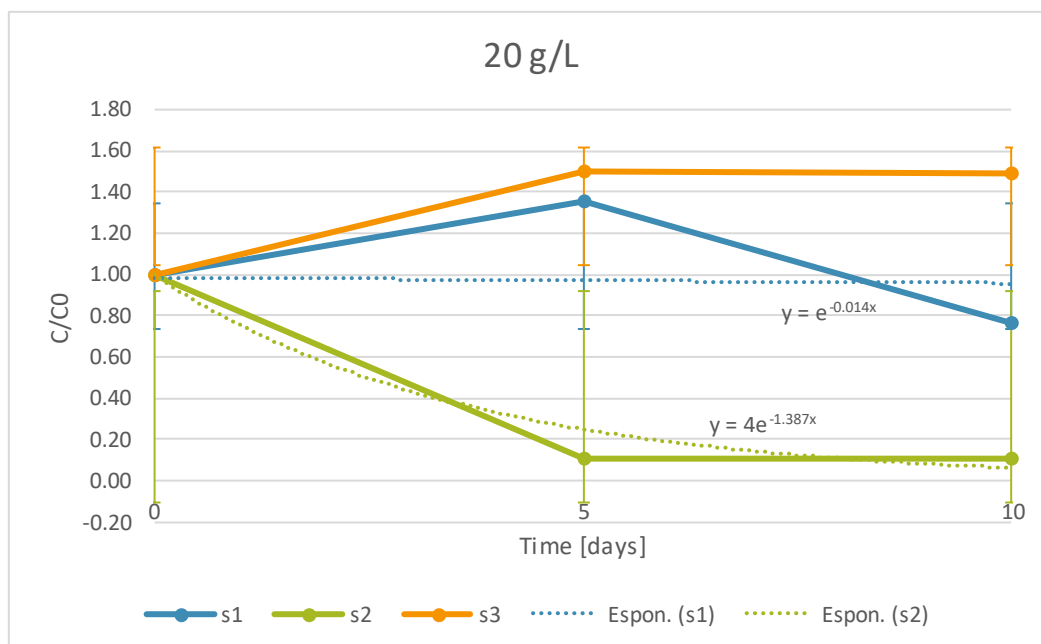


Figure 41 - PDS concentration profile for the three samples. PDS initial concentration 20 g/L

In order to compare PDS concentration values for 1 g/L and 20 g/L PDS initial concentration, bar charts were plotted for each soil. In this way, it was possible to understand the difference in order of magnitude in PDS concentrations, considering average values.

In Figure 42, PDS concentration was plotted in a log scale graph versus time, considering the experimental period after 5 and 10 days. Comparing the values for low and high PDS concentration (1 g/L and 20 g/L), for soil 1 PDS concentrations differ in both cases of one order of magnitude. The same situation is evident in the case of soil 2 in Figure 43. In the case of low PDS concentration (1 g/L) there is no significant difference in concentrations values. Figure 44 confirms the one order of magnitude difference in soil 3. Hence, an increase in the injected PDS concentration will enhance its persistence.

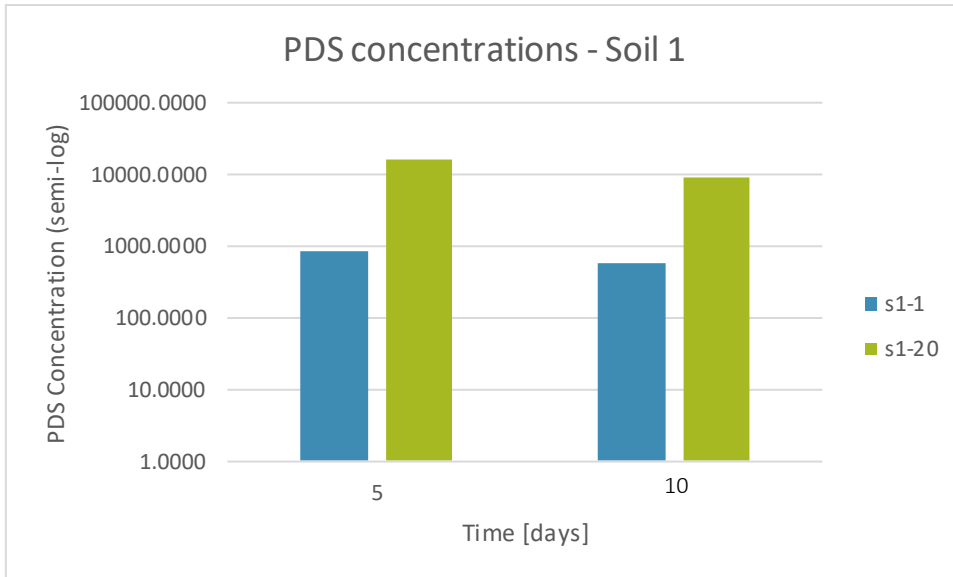


Figure 42 - PDS concentrations plotted in semi-log scale for soil 1 (s1) at low and high PDS initial concentration, 1 g/L and 20 g/L (1, 20)

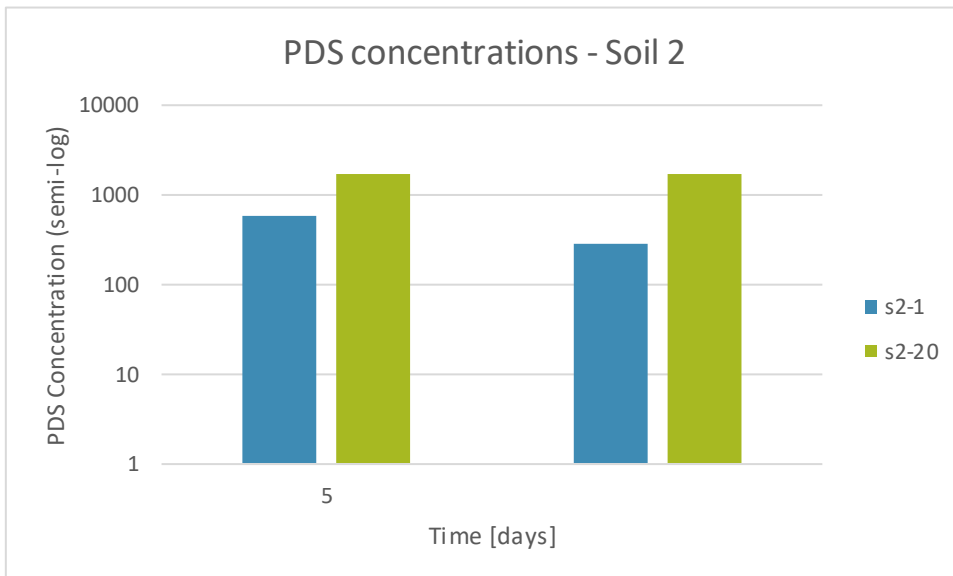


Figure 43 - PDS concentrations plotted in semi-log scale for soil 2 (s2) at low and high PDS initial concentration, 1 g/L and 20 g/L (1, 20)

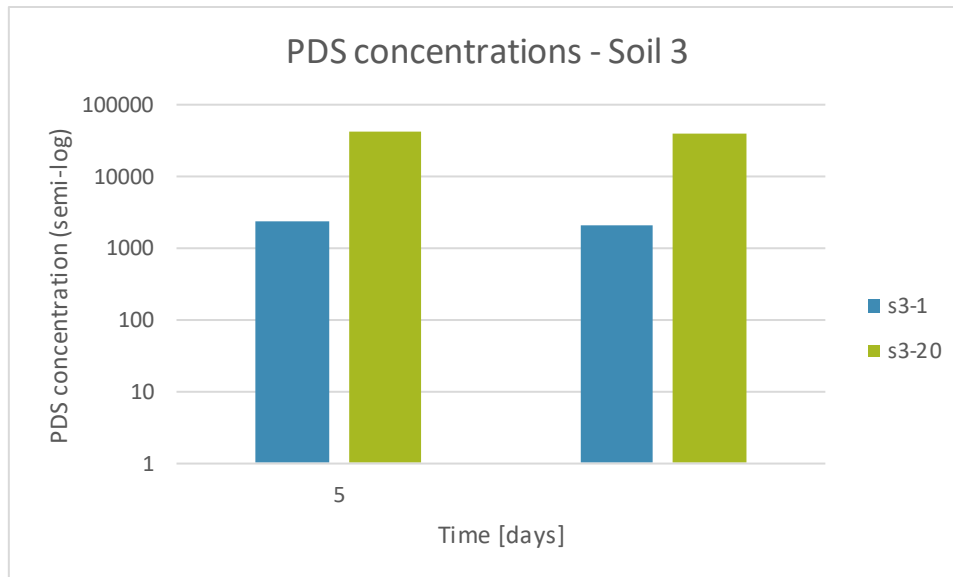


Figure 44 - PDS concentrations plotted in semi-log scale for soil 3 (s3) at low and high PDS initial concentration, 1 g/L and 20 g/L (1, 20)

#### 4.2.2.3 Sample reactors – SOD approach

In order to evaluate PDS decomposition, SOD concept was used and in detail reference was made to the oxidable matter analysis (related to the inorganic and organic components) and to the presence of iron and transition metals. Knowing that PDS oxidant demand is related to the decomposition due to the presence of soil organics and metals in the soil, it was possible to analyze this relation.

The impact of TOC content and the elemental composition was studied and the correlation between TOC versus  $k$  and Fe versus  $k$ , was analyzed.

Considering TOC percentage in both soil 1 and soil 2 and  $k$  values in the case of low PDS concentration (1 g/L), it was possible to obtain a relation between TOC content and decomposition rate. Figure 45 shows the presence of a high correlation between TOC and  $k$ , showing a coefficient of determination  $R^2$  of 0.9797.

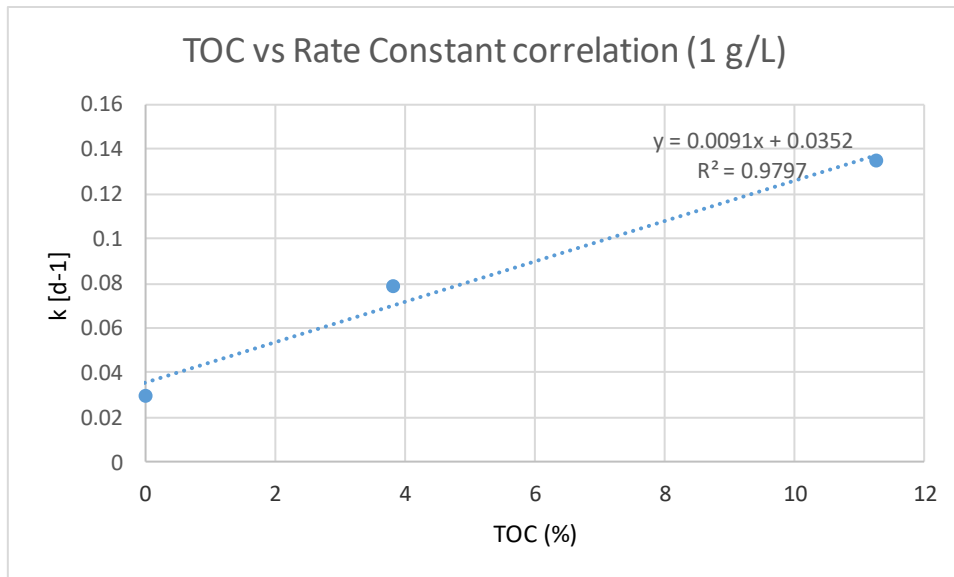


Figure 45- TOC vs k correlation for 1 g/L PDS concentration respectively for the three soils.

Taking into account the relation between Fe content and PDS decomposition, the correlation between Fe content and decomposition rate, for both low and high PDS concentration, was explored. As shown in Figure 46, Figure 47, a significant positive correlation was evident in the case of low PDS concentration (1 g/L), with a coefficient of determination  $R^2$  of 0.908. On the other hand, for the high concentration (20 g/L), the correlation was positive but insignificant.

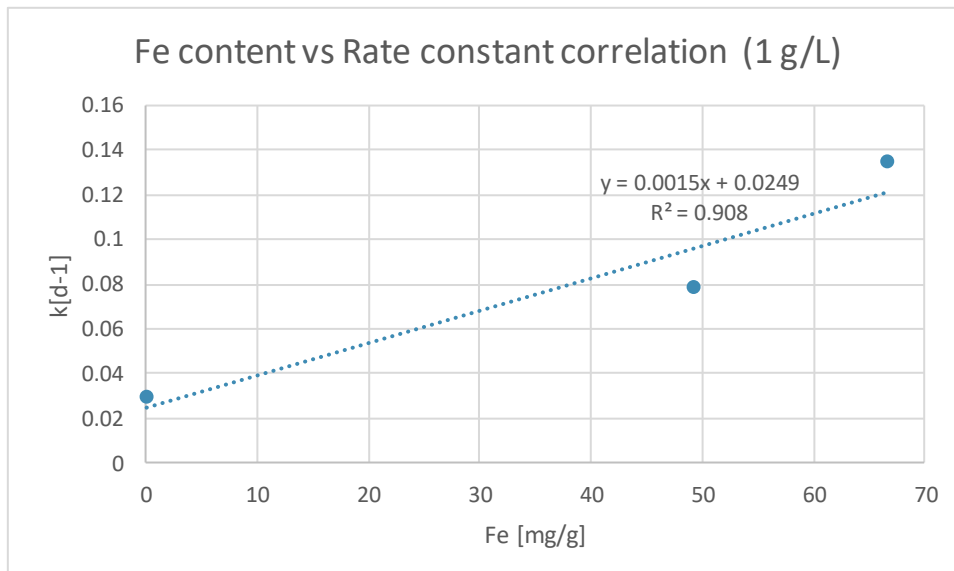


Figure 46 - Fe vs k correlation for 1 g/L PDS concentration respectively for the three soils.

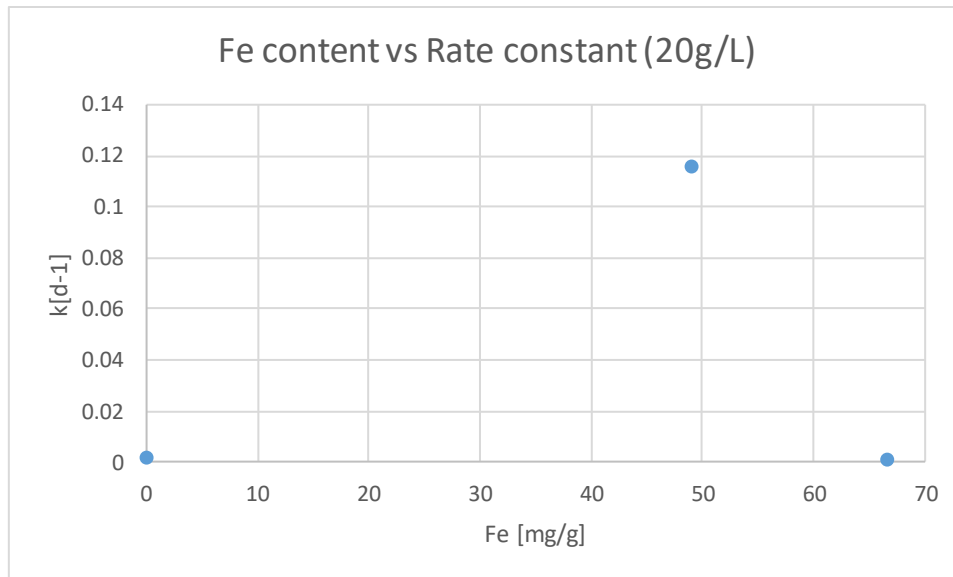


Figure 47 - Fe vs k correlation for 20 g/L PDS concentration respectively for the three soils.

For soil 2, the results shown a TOC content of ~ 12.86% and a contribution of Fe much greater than soil 1, with a maximum concentration of 66581 ppm. In this purpose it was evident that the PDS decomposition assumed very high value in term of velocity, due to the high concentration of Fe in soil that led to PDS decomposition. The rapid decrease in PDS concentration designated and confirmed that it is strongly related to TOC content and to the presence of heavy metals in the natural composition of the soils. Moreover, in this case, a rise in k was proportional to the increase of Mn content (3960 ppm), as shown in Figure 41, for low PDS concentration (1 g/L). Also in this case it was confirmed that PDS reacts with NOM and is depleted until sufficient oxidant is added to satisfy the oxidant demand <sup>37</sup>.

Sample 3, with high Si content, exhibited no PDS loss over 10 days. It was evident that the high Si content did not affect the rate of PDS decomposition. Moreover, the sample showed an absence in TOC and Fe content, leading the PDS to persist in soil in order to reach a hypothetical contaminant distance from the injection wells. The PDS in this case resulted very stable, with a high half-life.

In this purpose, considering soils 1 and 2 richer in TOC and Fe content, the results showed that their reaction with these compounds led to the consume of a high concentration of oxidant. Increasing levels of added PDS, its loss will continue to occur. This is the reason why the soils cited above are not perfectly suitable for PDS application. Due to the reactions between the oxidant and soil, the amount of PDS needed to be injected in the subsurface will increase. This

impact will have consequences also in term of costs of ISCO: if in some cases the NOD will be high enough, the use of PDS for this kind of soils will be uneconomical <sup>65</sup>.

### 4.3 Column experiments

Column experiments were performed in order to evaluate the evolution in time of PDS concentration considering high PDS concentration (20 g/L). PDS trend was compared between soil 1 and 3, in order to evaluate its behavior in two different soils.

For the column experiments, characterized by constant flow-rate (5 mL/min) and continuous injection of  $C_0 = \text{constant}$  in  $x = 0$ , the breakthrough curves were plotted using Ogata-Banks's solution (Eq.23) and the ratio  $C/C_0$  was evaluated over time.

For soil 3, as shown in Figure 48, for time > 20 min it is possible to approximate the behavior to a tracer, due to the absence of interaction between PDS and the porous medium, as in the case of batch-experiments. This trend can be related to the short time period in which PDS was in contact with the medium.

As illustrated in Figure 48, in the case of soil 1, the tendency of PDS to react is different: there was an increasing output concentration until the stability achievement describing an evident reaction between the oxidant and the components of soil.

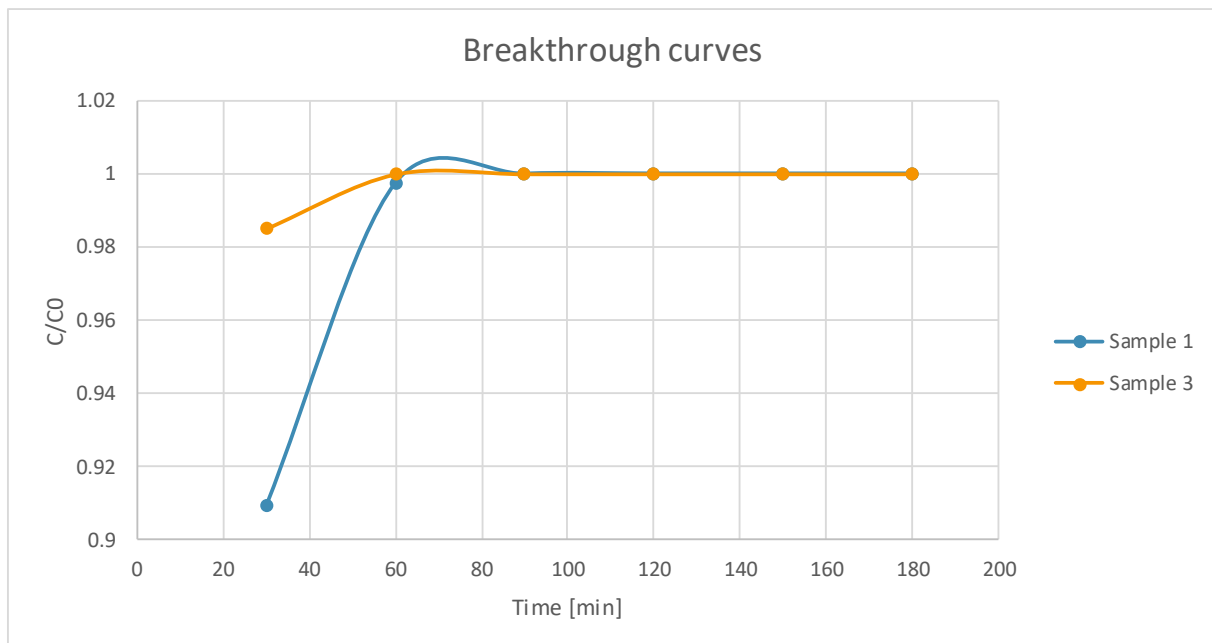


Figure 48 - Breakthrough curves related to PDS degradation

Comparing the results between column and batch experiments, it is noticeable that the duration is lower compared with batch tests. In the latter, the degradation was visible around some hours, whereas in column tests was evident a degradation of about ~ 30 min. No relationship between the batch and column was able to be developed about first-order degradation rate coefficient due to lack in data experiments.

Soil physical properties have a large impact on the capability of the soil to resist degradation. To better understand the initial soil characteristics of the tested samples, some experiments were performed.

The properties of the two analyzed samples are shown in Table 19:

*Table 19 - Porosity values ( $\epsilon$ ) for soil 1 and soil 3 calculated for column experiments considering the volume of water ( $V_w$ ) occupied into the pores and the total volume of the column ( $V_T$ )*

Parameter	Soil 1	Soil 3
$V_w$ [mL]	260	370
$V_T$ [mL]	724	724
$\epsilon$	0.36	0.51

The results show a higher porosity in the case of the sea sand (soil 3).

#### 4.4 Comparison with literature data

Based on different studies reported in the literature about PDS decomposition, it was possible to analyze some data in order to compare literature with the case explained above.

##### 4.4.1 Batch experiments

Sra et al. (2010) analyzed 7 aquifer materials across North America that presented different characteristics in term of TOC content, Fe and Mn as shown in Table 20:

*Table 20 - Aquifer materials characteristics and rate coefficient at low (1 g/L) and high (20 g/L) PDS concentration (Sra et al. (2010))*

Site	TOC [mg/g]	Fe [mg/g]	Mn [mg/g]	k (1 g/L) [d <sup>-1</sup> ]	k (20 g/L) [d <sup>-1</sup> ]
1	0.24	0.30	0.004	36.8	13.3
2	0.28	0.36	0.002	48.1	13.3
3	0.46	0.26	0.007	37.3	13.7
4	1.84	0.50	0.002	423.8	28.4
5	0.88	0.41	0.002	80.9	12.7
6	0.77	0.04	0.008	39.3	15.2
7	0.32	0.75	0.033	183.2	10.9

Based on these factors, it was possible to perform batch and column experiments in order to study PDS decomposition from a kinetic point of view. Compared with the 3 soils analyzed before, the 7 materials showed less TOC content and variable Fe content. On the other hand, Mn content was not available in sufficient quantity, so also in this case TOC and Fe content gave the major contribution in PDS decomposition.

As shown in Table 20, the decomposition rate coefficients showed in the paper, for low PDS concentration (1 g/L) were estimated to be higher compared to the high PDS concentration (20 g/L).

This consideration indicates that there was high stability at higher concentrations, confirmed also by the half-life values, shown in Table 21.

*Table 21 - Half-life Sra et al. (2010)*

Soil	Half-life [day]	
	Batch 1 g/L	Batch 20 g/L
<b>1</b>	188.2	521
<b>2</b>	144.2	521
<b>3</b>	186.7	505.5
<b>4</b>	16.4	243.9
<b>5</b>	85.7	546.9
<b>6</b>	176.3	457.3
<b>7</b>	37.8	637.2

As shown in chapter 4.2.2.2, the situation is consistent with the observations made above: less PDS is consumed and a higher half-life is showed in the case of high PDS concentration.

The k estimated for 1 g/L of PDS concentration, in this work resulted higher than three orders of magnitude compared with Sra et al. (2010) study and this result is related to the larger TOC content showed in the two soils from Czech Republic. In the case of 20 g/L PDS, k values were mostly similar in both studies, with an exception for the soil 1 of this investigation that showed a value of 0.1157 d<sup>-1</sup>.

From Table 20 and Table 21, considering rate coefficients and half-life of the different aquifer materials investigated, it is evident that the soil characterized by a lowest half-life for PDS concentration of 1 g/L, is the soil 4. It is characterized also by the highest TOC content (Table 20), that confirms the dependence of PDS decomposition on NOM.

For a major understanding, in their experiments Sra et al. (2010), studied the correlation between PDS decomposition rate and the parameters cited in Table 20. Concerning TOC content, as evident from Figure 49 and Figure 50, the study confirmed the high correlation with the estimated k. The significant positive correlation was showed by the coefficient of determination ( $R^2$ ) that for low and high PDS concentration was respectively 0.6679 and 0.8335.

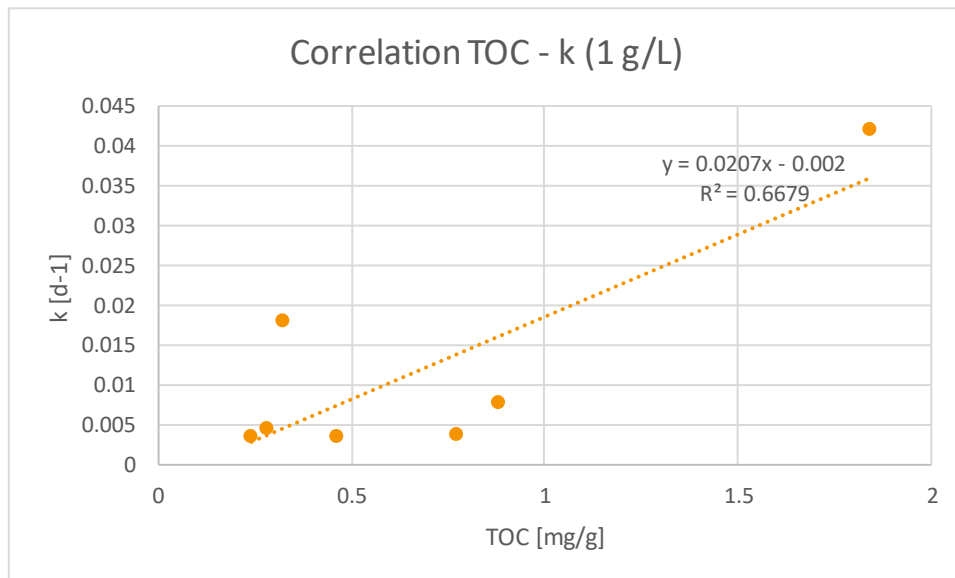


Figure 49 – TOC vs k correlation for 1 g/L PDS concentration (Sra et al. (2010))

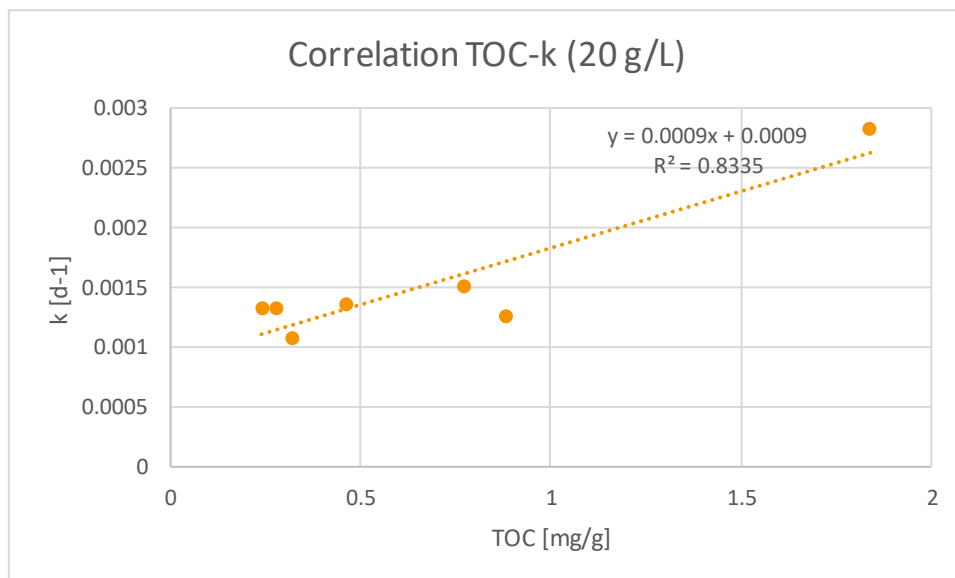


Figure 50 - TOC vs k correlation for 20 g/L PDS concentration (Sra et al. (2010))

Meanwhile there was an insignificant correlation between Fe, Mn content and k (Figure 51, Figure 52, Figure 53, Figure 54), with very low R<sup>2</sup> values for both PDS concentration, with an exception for Mn that for high PDS concentration showed a negative correlation.

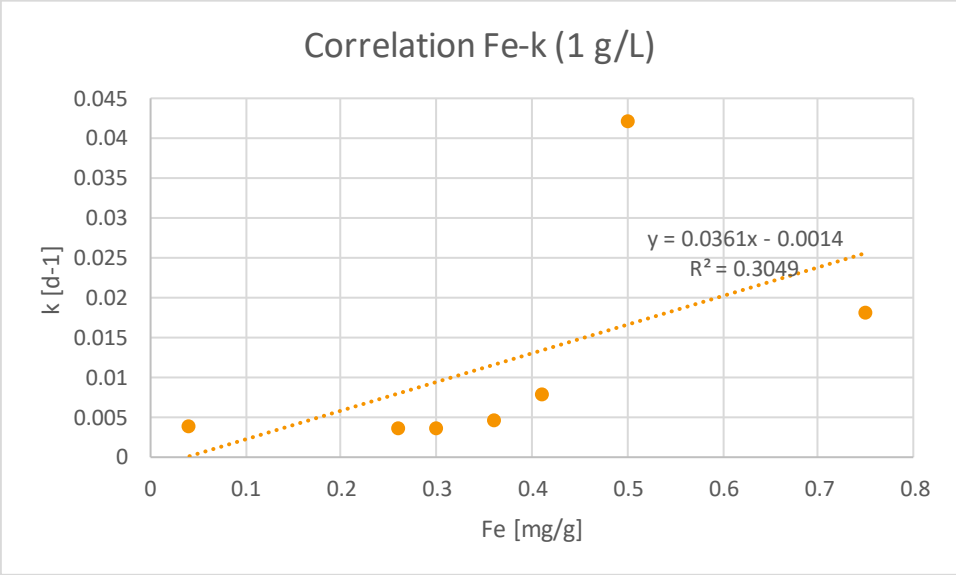


Figure 51 – Fe vs k correlation for 1 g/L PDS concentration (Sra et al. (2010))

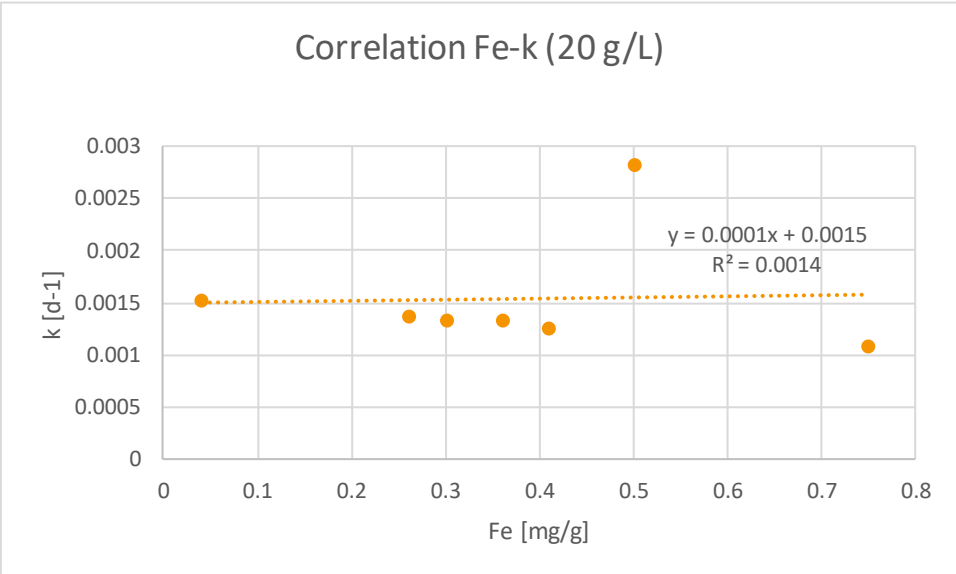


Figure 52 – Fe vs k correlation for 20 g/L PDS concentration (Sra et al. (2010))

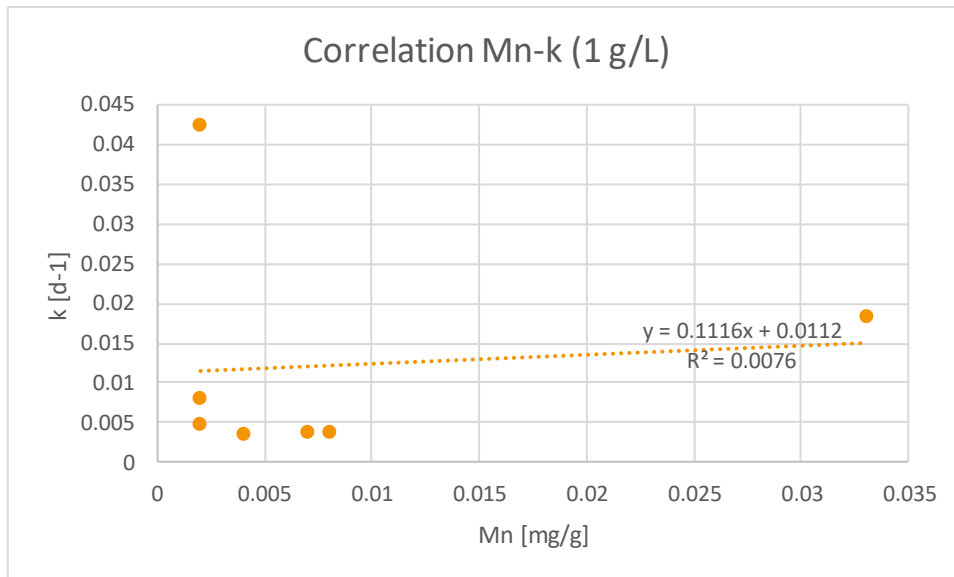


Figure 53 – Mn vs k correlation for 1 g/L PDS concentration (Sra et al. (2010))

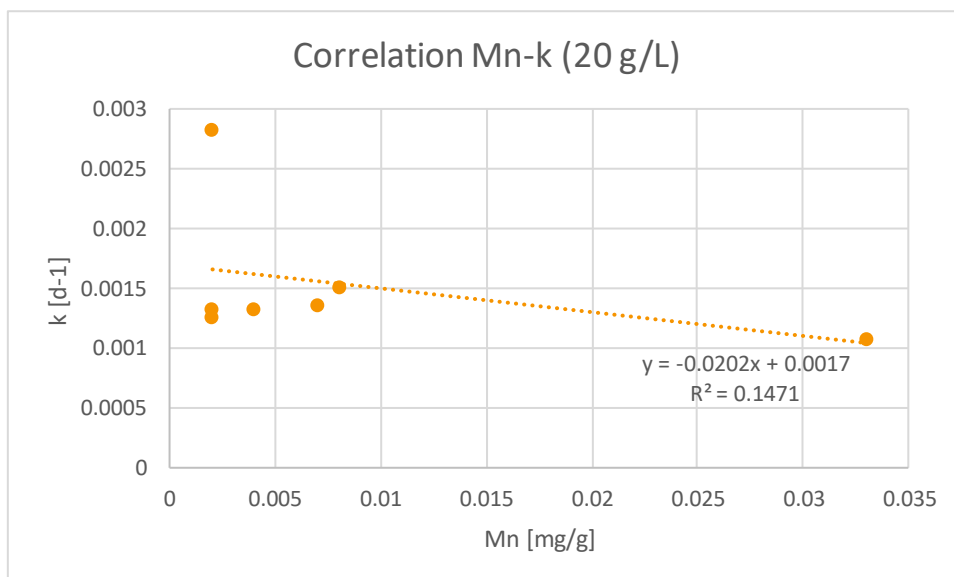


Figure 54 – Mn vs k correlation for 20 g/L PDS concentration (Sra et al. (2010))

Based on the similar operating conditions, the case of the soils from Czech Republic confirmed the correlation between TOC, Fe content and k, confirming that these factors are mainly responsible for oxidant decomposition and that give information about persistence, stability and transport of PDS in subsurface.

In addition, considering that PDS decomposition leads to H<sup>+</sup> production, Sra et al. (2010) observed changes of pH over time. In both low and high PDS concentration it was evident a decrease in pH as a result of the acidity generated. Moreover, the decrease was so much evident

in high PDS concentration due to the major production of H<sup>+</sup> caused by the higher PDS concentration <sup>67</sup>.

From the measures resulted that also TOC content had an impact on pH, indeed the material with the lowest TOC content showed the largest reduction of pH: in the case of low PDS concentration from 6.8 to 3.8 and for the high concentration from 8 to 1 <sup>67</sup>.

In this purpose, considering that PDS decomposition behavior was similar in both studies described, it can be expected the same pH trend also for soil 1 and 2 of this work (in both PDS concentration), where pH wasn't calculated. Therefore, an evident decrease in its values, with a major decrease for PDS concentration of 20 g/L. An exception may be evident in the case of control reactors and sea sand. In the first case due to the absence of aquifer materials and the nonappearance of reactivity with PDS, in the second case mainly for the poor or almost absent reaction with the oxidant.

Concerning the dependence of reaction rate on ionic strength, it is possible to relate the decrease in the rate coefficient to the increase in ionic strength of the solution <sup>67</sup>. No experiments were undertaken to analyze the ionic strength in both literature and this work studies, but it is expected that some dissolved metals (Fe, Mn) would contribute to a rise in ionic strength values over time as PDS decomposes.

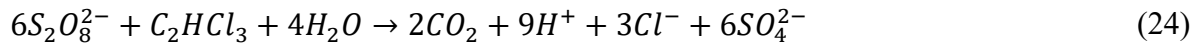
SOD approach was used in other studies in order to relate the PDS demand of different soils. Particularly, Brown et al. (2004) in their studies analyzed SOD in different soils obtaining the results shown in Table 22<sup>65</sup>:

*Table 22 - SOD tests Brown et al. (2004)*

<b>Soil</b>	<b>SOD (g/kg)</b>
<b>Silt</b>	< 0.05
<b>Sand, high TOC content</b>	6.45

As an example, it was simulated a real case knowing SOD in sand. If 1 m<sup>3</sup> of soil is treated using PDS and in this soil TCE is present, it is necessary to consider that an amount will be consumed by soil and another part will be available for the contaminant degradation. Calculating the amount of PDS available after the consumption due to the soil components, it is possible to evaluate the quantity of TCE that can be degraded. It was assumed to use two

doses of peroxydisulfate ion ( $S_2O_8^{2-}$ ): 10 g/kg and 20 g/kg. Considering that in the case of a sand with high TOC content the consume of PDS is equal to 6.45 g/kg, as shown in Table 23 and considering the reaction between  $S_2O_8^{2-}$  and TCE (Eq.24), the evaluation was conducted.



With a dose of 10 g/kg, only 3.55 g/kg of PDS are available for TCE oxidation. Knowing the molecular weight of PDS (192.123 g), it was possible to evaluate the number of moles. The moles that can be used to degrade TCE were 0.018 mol, therefore 0.0061 mol of TCE can be oxidized using 10 g/kg of PDS. Using a dose of 20 g/kg and following the procedure above, it resulted that 0.023 mol of TCE can be degraded.

Considering that for ISCO applications sodium peroxydisulfate is used, it is necessary to consider a higher number of moles.

#### 4.4.2 Column experiments

In order to make a comparison between the column experiments in Sra et al. (2010) study and this work, breakthrough curves were simulated using Bear's solution (Eq.25). The equation needs the knowledge of some parameters that permit to calculate the behavior of PDS changes over time. Particularly, knowing the column and soils characteristics (Table 23, Table 24), plus the degradation coefficients, the ratio  $C/C_0$  was estimated for 20 g/L of PDS concentration. In order to make the comparison, the solution was calculated only for the soils with high and less TOC content, respectively soil 4 and 1.

Table 23 - Column properties

Column		
Lenght [cm]	Diameter [cm]	Flow-rate [mL/min]
40	5	8

Table 24 - Porosity values

Porosity	
1	0.82
2	0.82
3	0.8
4	0.32
5	0.36
6	0.32
7	0.77

Effective velocity ( $v_{eff}$ ) was estimated as the ratio between Darcy's velocity (knowing the flow rate and the column section) and porosity, the time requested to fill all the column's pore was ~ 20 min.

The breakthrough curves (Figure 55) showed that PDS in time had a similar trend with the curves estimated in laboratory. Particularly, soil 1 (< TOC content) showed the first appearance of PDS in the column effluent after 20 min. After breakthrough, the concentration slowly increased, until it reached stationarity conditions ( $C/C_0 = 0.84$ ). The slow change in PDS concentration over time confirmed, also in this case, the low reaction between soil with low TOC content and PDS.

In soil 4 (> TOC content) PDS concentration was evident after 20 min, but in this case the steady-state conditions achievement was faster ( $C/C_0 = 0.90$ ). In this case PDS behaved like a tracer: more time would be necessary to observe a change in PDS concentration.

From the column data resulted that PDS decomposition rates can be represented by a first-order kinetic law, but the values were higher than the corresponding batch  $k_{obs}$  results, indicating a strong sensitivity of reaction rates to the oxidant to aquifer solids mass ratio<sup>67</sup>. The high  $k_{obs}$  values in soil 4 (Figure 55) confirmed the low stability of PDS due to the low half-life estimated and a higher transport velocity.

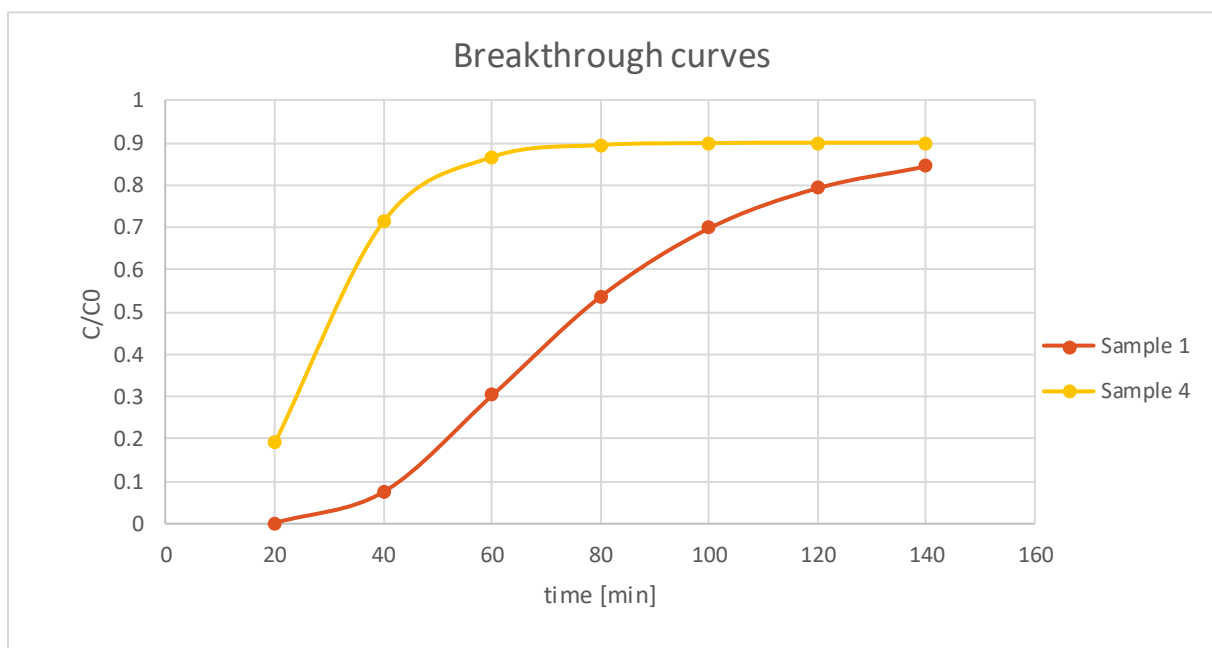


Figure 55 - Breakthrough curves from Sra et al. (2010) studies

## 5 Conclusions

The goal of this work was to understand the persistence and stability of unactivated PDS using three different aquifer materials. PDS decomposition was evaluated using batch and column experiments.

In batch experiments the decomposition was investigated analyzing the degradation rate coefficients and half-life values during the entire experimental period (~ 10 days) using low (1 g/L) and high (20 g/L) PDS concentration. The results were related to the soil parameters and showed that PDS decomposition followed the first-order rate law and that it depended mostly on TOC and Fe content. Particularly, for low PDS concentration the values of the decomposition rate coefficient ( $k$ ) were higher compared with high PDS concentration, showing a greater PDS stability for high concentration. A high influence of initial concentration on  $k$  was evident and may be attributed to a pseudo first-order rate law. In the sea sand, that showed a high Si content but no TOC and Fe traces, there was an evident stability due to the absence of elements that could react with the oxidant.

Moreover, literature results showed that PDS degradation leads to the reduction in pH due to the production of  $H^+$ . Particularly, this reduction was so much evident in the case of high PDS concentration due to the high production of  $H^+$ . For this reason it is fundamental to analyze pH drop before design ISCO treatment, in order to consider factor that could decrease PDS persistence in soil <sup>2</sup>.

Column experiments were analyzed simulating breakthrough curves in time and studying the variation in PDS concentration for two soils (one with visible Fe content and one sea sand). The results showed that in the case of sea sand, with no TOC and Fe content, the PDS concentration rapidly reached the influent concentration, highlighting the absence of PDS decomposition. On contrary, the soil with high Fe and TOC content showed an evident mass transfer due to the rise in PDS concentration, followed by a stationary condition ( $C/C_0 = 1$ ). The  $k$  observed by Sra et al. (2010) during column experiments was higher compared to those observed in this study. The main reason that is evident also from our experiments is the different composition of soil matrix that heavily impaired the PDS decomposition

According to the literature, both experiments demonstrated the high dependence of unactivated PDS stability on soil properties (TOC and Fe content). This trend was confirmed studying the correlation between  $k$  and soil properties. The results showed that  $k$  estimated for low and high PDS concentration experiments are strongly correlated with the TOC and Fe content.

The knowledge of PDS persistence would permit advective and diffusive transport, facilitating the transport of PDS in areas further away from the injection wells. In this way it would be possible to treat larger contaminated areas with one injection. Moreover, the study on stability would exclude the use of PDS in soils with specific characteristics that would increase PDS demand. In the cases in which soils are not suitable for PDS applications, the amount of the oxidant will quickly decrease and in this way its amount will not be available for contaminants oxidation. In this purpose, it is important to know specific parameters as TOC and Fe content of soil, that would permit to evaluate in detail SOD and the effective costs for oxidant delivery. Indeed, when the impact of SOD is considered PDS costs become considerable. As a result, PDS will be suitable for contaminated soils with controlled TOC and Fe content <sup>5</sup>.

## 6 References

1. Mahmood, AN, Mahmood, JA, Alabbasy, AJ, et al. A Literature Review on Types of Contamination (Biological, Chemical, Medical). *Journalpub* 2019:9.
2. Pérez, AP, Eugenio., NR. Status of local soil contamination in Europe. *Publications Office of the European Union*; 2018:193.
3. Stolte, J, Tesfai, M, Øygarden, L, et al. *Soil threats in Europe*. 2016:13.
4. Panos, P, Van, LM, Yusuf, Y, et al. Contaminated Sites in Europe: Review of the Current Situation Based on Data Collected through a European Network. *Journal of Environmental and Public Health* 2013;Volume 2013:11.
5. Liedekerke, MHV, Gundula, P, Sabine, R-B, et al. Progress in the Management of Contaminated Sites in Europe. *ResearchGate*; 2014:73.
6. Farrington, JW. Chlorinated Hydrocarbons. *Encyclopedia of Ocean Sciences* 2001.
7. Honetschlägerová, L, Martinec, M, Škarohlíd, R. Coupling in situ chemical oxidation with bioremediation of chloroethenes: a review. *Reviews in Environmental Science and Biotechnology* 2019;18(4):699-714.
8. Olaniran, AO, Pillay, D, Pillay, B. Chloroethenes contaminants in the environment: Still a cause for concern. *African Journal of Biotechnology* 2004;Vol. 3 (12):8.
9. B.H.Kueper, P, G.P.Wealthall, D, J.W.N.Smith, et al. An illustrated handbook of DNAPL transport and fate in the subsurface. *Environment Agency*; 2003:67.
10. Integrated Risk Information System (IRIS) on Tetrachloroethylene.; 2012. Accessed.
11. Watson, AloopRE, Jacobson, CF, Williams, AL, et al. Trichloroethylene-contaminated drinking water and congenital heart defects: A critical analysis of the literature. 2006.
12. Joseph A. Cichocki, Kathryn Z. Guyton, Neela Guha, et al. Target Organ Metabolism, Toxicity, and Mechanisms of Trichloroethylene and Perchloroethylene: Key Similarities, Differences, and Data Gaps. *THE JOURNAL OF PHARMACOLOGY AND EXPERIMENTAL THERAPEUTICS* 2016:14.
13. Toxicological profile for Tetrachloroethylene; 2019. Accessed.
14. TCE and PCE Toxicity, Uses, and Properties; Accessed.
15. Dolinová, I, Štrojsová, M, Černík, M, et al. Microbial degradation of chloroethenes: a review. *Springer-Verlag Berlin Heidelberg* 2017:22.
16. Benson, B. 1,1-DICHLOROETHENE (VINYLIDENE CHLORIDE). *World Health Organization*; 2003.
17. Li, D, Liu, S. Groundwater Quality Detection. *Water Quality Monitoring and Management* 2019.
18. Jayaraj, R, Megha, P, Sreedev, P. Organochlorine pesticides, their toxic effects on living organisms and their fate in the environment. 2016.
19. Dai, Q, Min, X, Weng, M. A review of polychlorinated biphenyls (PCBs) pollution in indoor air environment. 2016.
20. Faroon, O, Ruiz, P. Polychlorinated biphenyls: New evidence from the last decade. 2016.
21. Pocar, AloopP, i, TALB, Antonini, S, et al. Cellular and molecular mechanisms mediating the effect of polychlorinated biphenyls on oocyte in vitro maturation. *Reproductive Toxicology* 2006.
22. Mitra, S, Roy, P. BTEX: a serious ground-water contaminant. *Environmental Sciences* 2011:6.

23. M., BP. Microbial degradation of chloroethenes in groundwater systems. *Hydrogeology Journal* 1999:8.
24. Robert L. Siegrist, Michelle Crimi, Brown, RA. *In Situ Chemical Oxidation: Technology Description and Status*. Springer New York, 2011.
25. Spruit, B, Cuni, LL. *Soil Remediation Techniques: Examination of In Situ Chemical Oxidation. Geoenvironmental Engineering Remediation Technology*. 2015.
26. Watts, R, Teel, A, Brown, R, et al. Field Demonstration, Optimization, and Rigorous Validation of Peroxygen-Based ISCO for the Remediation of Contaminated Groundwater - CHP Stabilization Protocol. 2014:99.
27. Siegrist, RL, Crimi, M, Simpkin, TJ. *In Situ Chemical Oxidation for Groundwater Remediation*. 2011.
28. Molfetta, AD, Sethi, R. *Ingegneria degli Acquiferi*. Springer, 2012.
29. Speight, AloopJG. *Redox Transformations. Reaction Mechanisms in Environmental Engineering* 2018.
30. Xu, X, R.Thomson, N. A long-term bench-scale investigation of permanganate consumption by aquifer materials. 110. *Journal of Contaminant Hydrology*; 2009:73-86.
31. Urynowicz, MA, Balu, B, Udayasankar, U. Kinetics of natural oxidant demand by permanganate in aquifer solids. *Journal of Contaminant Hydrology* 2007:8.
32. Renato, B. *Principles, Developments and Design Criteria of In Situ Chemical Oxidation*. Springer Science; 2013:11.
33. Crimi, AloopM, Ko, S. Control of manganese dioxide particles resulting from in situ chemical oxidation using permanganate. *Chemosphere* 2009.
34. Urynowicz, MA, Crimi, M. Genesis and Effects of Particles Produced during In Situ Chemical Oxidation Using Permanganate. *Journal of Environmental Engineering* 2002:13.
35. Bo-Tao Zhang, Yang Zhang, YT, Fan, M. Sulfate Radical and Its Application in Decontamination Technologies. *Critical Reviews in Environmental Science and Technology*, 2014:46.
36. i, AloopHC, Lim, H-N, Kim, J, et al. Transport characteristics of gas phase ozone in unsaturated porous media for in-situ chemical oxidation. *Journal of Contaminant Hydrology* 2002:8.
37. Fang, G, Chen, X, Wu, W, et al. Mechanisms of Interaction between Persulfate and Soil Constituents: Activation, Free Radical Formation, Conversion, and Identification 2018:10.
38. Evans, PJ, Dugan, P, Nguyen, D, et al. Slow-release permanganate versus unactivated persulfate for long-term in situ chemical oxidation of 1,4-dioxane and chlorinated solvents. *Chemosphere* 2019;221:802-811.
39. TSITONAKI, A, PETRI, B, CRIMI, M, et al. *In Situ Chemical Oxidation of Contaminated Soil and Groundwater Using Persulfate: A Review Critical Reviews in Environmental Science and Technology* 2010:38.
40. O L H A S . F U R M A N , L, AMYLTEE, S, RICHARDJWATT. Mechanism of Base Activation of Persulfate. 44. *ENVIRONMENTAL SCIENCE & TECHNOLOGY*; 2010:6.
41. H., WR, G., TP, L., JR, et al. Oxidation of Chlorinated Ethenes by Heat-Activated Persulfate: Kinetics and Products. *Environ. Sci. Technol*; 2007:6.
42. Wanga, J, Wanga, S. Activation of persulfate (PS) and peroxymonosulfate (PMS) and application for the degradation of emerging contaminants *Chemical Engineering Journal* 2018:16.

43. AIKATERINI TSITONAKI , BENJAMIN PETRI , MICHELLE CRIMI , et al. In Situ Chemical Oxidation of Contaminated Soil and Groundwater Using Persulfate: A Review *Critical Reviews in Environmental Science and Technology* 2010:38.
44. Gong, JLX, Song, S, Zhang, F, et al. Heat-Activated Persulfate Oxidation of Chlorinated Solvents in Sandy Soil *Journal of Spectroscopy*; 2014:6.
45. Zhaoa, D, Liaob, X, Yanb, X, et al. Effect and mechanism of persulfate activated by different methods for PAHs removal in soil. *Journal of Hazardous Materials* 2013:8.
46. Wei, Z, Villamena, FA, Weavers, LK. Kinetics and Mechanism of Ultrasonic Activation of Persulfate: An in Situ EPR Spin Trapping Study *Environmental Science and Technology*; 2017:8.
47. Deng, D, Lin, X, Ou, J, et al. Efficient chemical oxidation of high levels of soil-sorbed phenanthrene by ultrasound induced, thermally activated persulfate. *Chemical Engineering Journal* 2015:8.
48. Li, Y-T, Li, D, Lai, L-J, et al. Remediation of petroleum hydrocarbon contaminated soil by using activated persulfate with ultrasound and ultrasound/Fe *Chemosphere* 2020:8.
49. Matzek, LW, Carter, KE. Activated persulfate for organic chemical degradation: A review. *Chemosphere* 2016:11.
50. Domingueza, CM, Rodriguezb, V, Monterob, E, et al. Abatement of dichloromethane using persulfate activated by alkali: A kinetic study. *Separation and Purification Technology* 2020:9.
51. Wilsona, S, Farone, W, Leonardc, G, et al. Advancing In Situ Chemical Oxidation (ISCO) Technology. *Regenesi*; 2013:16.
52. Lin, Y-T, Liang, C, Chen, J-H. Feasibility study of ultraviolet activated persulfate oxidation of phenol. *Chemosphere* 2011:5.
53. Yong-qing, Z, Xiao-fang, X, Shao-bin, H, et al. Effect of chelating agent on oxidation rate of aniline in ferrous ion activated persulfate system at neutral pH. Springer; 2014:7.
54. Sra, KS, Thomson, NR, Barker, JF. Stability of Activated Persulfate in the Presence of Aquifer Solids. *Soil and Sediment Contamination: An International Journal* 2014:19.
55. Fang, M, Mao, M, Wen, Z. Degradation of phenol in water by Fe(II)-citrate activated persulfate oxidation *Earth and Environmental Science*. 2019:7.
56. Liang, C, Bruell, CJ, Marley, MC, et al. Persulfate oxidation for in situ remediation of TCE. II. Activated by chelated ferrous ion *Chemosphere* 2004:9.
57. Liu, H, Bruton, TA, Doyle, FM, et al. In Situ Chemical Oxidation of Contaminated Groundwater by Persulfate: Decomposition by Fe(III)- and Mn(IV)-Containing Oxides and Aquifer Materials. 2014:8.
58. Liang, C, Huang, C-F, Chen, Y-J. Potential for activated persulfate degradation of BTEX contamination *Science Direct*; 2008:10.
59. Liu, N, Ding, F, Weng, C-H, et al. Minimizing the interference of carbonate ions on degradation of SRF3B dye by Fe<sup>0</sup>-aggregate-activated persulfate process. *Separation and Purification Technology* 2016;169:230-240.
60. Bennedsen, LR, Muff, J, Sogaard, EG. Influence of chloride and carbonates on the reactivity of activated persulfate. *Chemosphere* 2012;86(11):1092-1097.
61. Liang, C, Wang, Z-S, Mohanty, N. Influences of carbonate and chloride ions on persulfate oxidation of trichloroethylene at 20 °C. *Science of The Total Environment* 2006;370(2):271-277.
62. Stathoulopoulos, A, Mantzavinos, D, Frontistis, Z. Coupling Persulfate-Based AOPs: A Novel Approach for Piroxicam Degradation in Aqueous Matrices. *Water* 2020;12:1530.

63. *Suthersan, SS, Horst, J, Schnobrich, M, et al. Remediation Engineering. 2 ed., 2017.*
64. Liang, C, Chien, Y-C, Lin, Y-L. Impacts of ISCO. Persulfate, Peroxide and Permanganate Oxidants on Soils: Soil Oxidant Demand and Soil Properties, Soil and Sediment Contamination Soil and Sediment Contamination: An International Journal 2012:21.
65. Brown, RA, Robinson, D, Skaldany, G, et al. Response to naturally occurring organic material: Permanganate versus persulfate. Germany; 2003:109.
66. First-order reactions; 2020. Accessed.
67. Sra, KS. Persulfate Persistence and Treatability of Gasoline Compounds Waterloo, Ontario, Canada: University of Waterloo; 2010:171.
68. PeroxyChem. Persulfate Oxidant Demand. Peroxygen Talk; 2007.
69. Guthrie, JM. Overview of X-ray Fluorescence; 2012. Accessed.
70. Fluorescence, X-XR. Accessed.
71. Paula, PAd. Physical Chemistry for the Life Sciences. 2010.
72. Barwick, V. Preparation of Calibration Curves. LGC Limited 2003. 2003.
73. Li, Y, Yang, K, Liao, X, et al. Quantification of Oxidant Demand and Consumption for In Situ Chemical Oxidation Design: in the Case of Potassium Permanganate. Water, Air, & Soil Pollution 2018;229.